

Responses to Anonymous Referee #1

Below the review is reproduced in black font and our responses interspersed in blue.

Comments:

The paper describes a new configuration of a regional coupled ocean-circulation biogeochemical model. The focus is on simulating the variability of oxygen. The main point of the paper is the description of the simulated interplay of biogeochemical processes, oceanic circulation and air-sea gas exchange which results in a variability of pelagic oxygen concentrations.

I see two routes the paper could go from there to be of interest to the wider audience addressed by Biogeosciences:

(1) Highlight one (or more) process which you have identified in your model and which have not been thought about in the past (in the literature). (I guess my main point here is that your "new" science is not easy to recognize. A good example is your abstract where the reader is left wondering which of the processes have been "discovered" by the authors.)

Reply: We believe we show in our revision what the new insights and contributions of this study are. We appreciate the Reviewer making this point and forcing us to clarify and emphasize this.

(2) Convince the reader that your model simulation is a realistic copy of reality.

Reply: We added a dedicated section on Model validation (2.1) to the revised manuscript where we included information that was previously located in the Supplement and also added a comparison of nitrate. Overall, we present model-data comparisons for surface and bottom temperature (satellite and in-situ) and salinity (in-situ), simulated current patterns and strengths (qualitative and observation and model derived numbers from previous literature), chlorophyll (satellite), and surface nitrate and bottom oxygen (both in-situ) and report correlation coefficients for these comparisons.

In its present form, I got the impression that the manuscript apparently has chosen route (2). The problem I have with this is: the only observations presented that give an impression of the model's fidelity are the oxygen data in Fig. 2. It is not very much data and the fit is not very good either. The overall correlation is 0.76 so your model explains less than 60% of the variance (of which a considerable fraction may be associated to the seasonal cycle meaning that the correlation in each subpanel of Fig. 2 is probably much less.) For comparison: global models are well above 0.8 for nutrients (e.g. Laufkoetter et al. 2015 their Fig. 1) and even for oxygen (e.g. Matear & Lenton 2014 their Fig. 1).

Reply: We are not sure that we agree with the Reviewer's assessment that this manuscript has to choose either route (1) or (2). We believe we are presenting new insights into the oxygen dynamics of the ECS and are doing so with a new model set-up that we believe to be superior to previous models published for the region and that is validated as rigorously as possible given the limited availability of observations. We don't think that a comparison of our model's correlation coefficient with those from global models is meaningful.

In order to give the reader a chance to put your model results into perspective I suggest that you extend you model evaluation section - preferably with in-situ measurements of nutrients, temperature and salinity (and/or sea surface temperature, chlorophyll, sea surface height estimated from space).

Reply: Done, see [previous comment](#).

Responses to Anonymous Referee #2

Below the review is reproduced in black font and our responses interspersed in blue.

Comments:

This publication presents a numerical model study of the hypoxia events off the Changjiang Estuary.

The combination of the different modeling components is a priori convincing and appropriate: 3D oceanic circulation model, biogeochemical model, sedimentary oxygen consumption module, river discharge (nutrient and freshwater load), and atmospheric forcing from reanalysis.

My main concern is about the model validation or skill evaluation before any use.

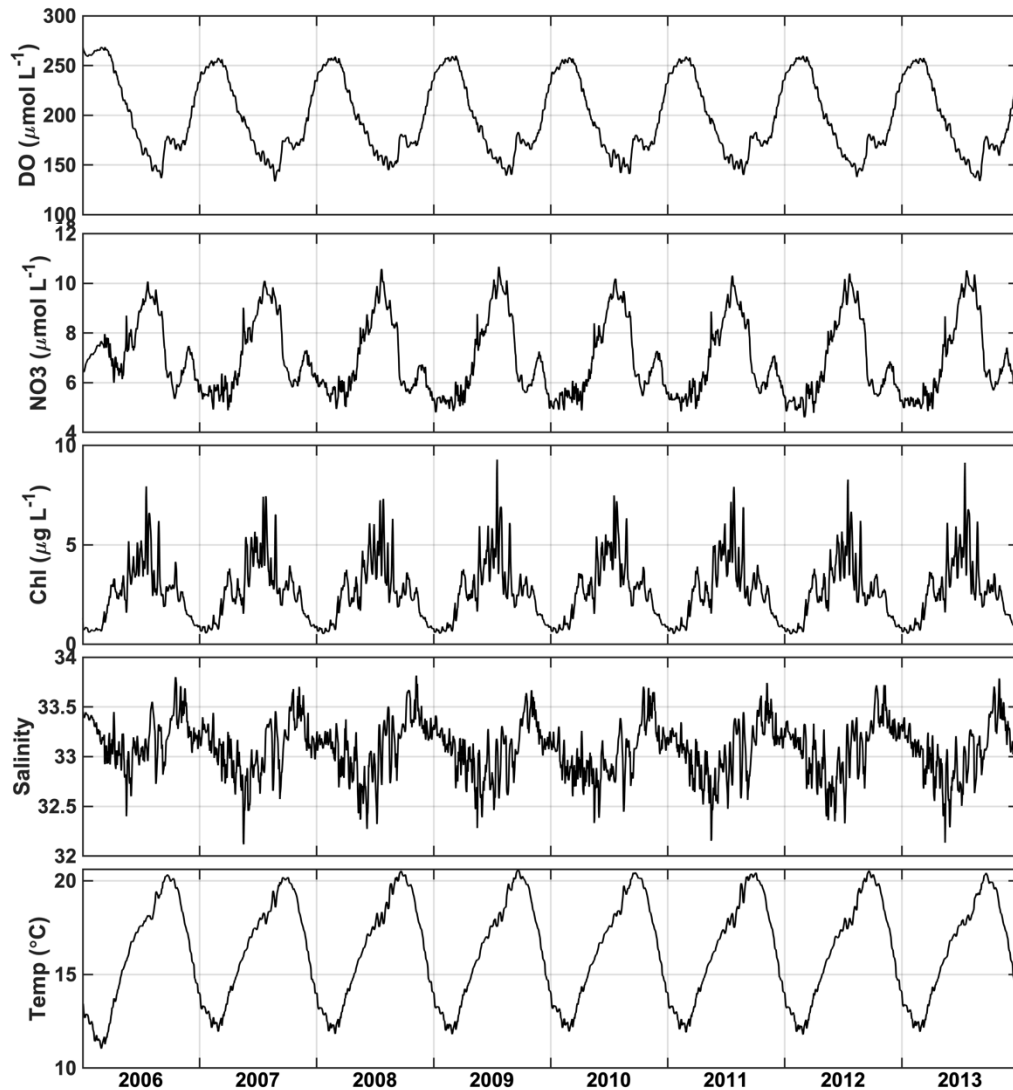
Reply: We appreciate this overall positive assessment and believe we have addressed the Reviewer's concerns regarding model validation as described in more detail below.

The model-data comparison is presented in section 3.1, Figure 2 only, and some other in the Supplement. The display of Figure 2 is problematic: color points (data) having the same color (same value) as the background (the model) do not appear. It is really difficult to see the observational structure and to evaluate the agreement with the model. (same for Figures S2, S3, S4). It could be separated figures (data distribution and model). Figure S6, including the bottom line, is much more speaking.

Reply: We have added a dedicated model-data comparison section (2.1) and a comparison for nitrate to illustrate that the model reproduces nutrient distributions well. Also, we agree with the Reviewer that the data points were blending in the background and have replotted the comparison figures for the in-situ observation comparisons in better quality and in colourblind-friendly scales. We are happy that the Reviewer finds the 2D histograms in Figure S6 (see also Figure S1) informative. These graphs only make sense when a large number of data points is available (usually only the case for satellite data). For the comparisons with in-situ observations we included correlation coefficients.

The authors aim at reproducing the observations from 9 cruises from march 2011 to september 2013. Therefore, the simulation starts in 2006, uses climatological observations from this period to force the model, 2006-2007 are used as spin-up, and the model is run in 2008-2013 for analysis. Regional models may be very dependant on the boundary conditions. Nothing is demonstrated about the robustness of the inner region : is there any drift in the total budgets (nutrients, oxygen, intensity of the Primary Productivity) ? The model is set and used. I would be more confident with the results if any sensitivity test would be performed. By example, it would be possible to run the model for the same duration (8 years) but with repeating the same annual forcing (e.g. 2006), in order to control that the inner structure of the PP and hypoxia are repeated or if any trend exist. It would also evaluate the model-internal-variability, not to be confused with the variability induced by the varying forcing (winds, river discharge).

Reply: We are confident that there is no drift in the domain. Following the Reviewer's suggestion, we have conducted an 8-year climatological simulation where the 2006 forcing was repeated year after year. Shown below is the mean bottom oxygen concentration and surface chlorophyll, nitrate, temperature and salinity in the region affected by hypoxia. We hope it is obvious that there is no drift and that the system is in dynamic steady state. Also, we appreciate the Reviewer's suggestion to contrast the original simulation with realistic forcing with the climatological simulation that repeats the same forcing every year; however, given the plot below, which shows that the results are essentially identical from year to year (except for some random fluctuations) we believe this is not necessary or instructive.



The model is used in its "optimal" configuration, but the evaluation to reach to this configuration is not presented. The model here is not used to make any sensitivity experiment. Part of this is explained late in the paper (line 384, just before the conclusion): there is a companion paper (Grosse et al.) that presents modeling experiments to quantify the relative importance of the processes responsible for hypoxia. This is important since the authors just infer the importance of

processes (lines 325-334), without proceeding to the sensitivity test to their hypotheses. In this case, I would indeed recommend to proceed to a simulation while removing the nutrient load (which seems to be done in the companion paper). It should be presented from the beginning that part of the modeling analysis is done somewhere else.

Reply: We now refer to the companion paper by Grosse et al. also in the Introduction. We are not presenting nutrient load reduction experiments in this manuscript. Some are presented in the companion paper by Grosse et al. A more extensive analysis of nutrient load reduction experiments is the subject of a forthcoming manuscript led by Arnaud Laurent.

Concerning the main conclusions of the publication, the analysis of the main contributors to hypoxia, in the whole water column and in the bottom layers, is relevant. It is important to be able to evaluate the relative importance of Water Respiration versus Sedimentary oxygen consumption. But once again, data are missing, or at least a more rigorous model-data evaluation. As an example: Figure 3 focuses on the patterns of the hypoxia events from 2008 to 2013, and different behaviors or chronology could be distinguished (that is very interesting in itself, and the modeling tool is really appropriate for this kind of studies). Unfortunately, it is insufficiently documented, how does this relate to observations ? Same for the discussion about the influence of wind events (4 typhoons) on the hypoxia extent.

Reply: We appreciate the Reviewer's assessment that one of our main conclusions about the contributions of water column versus sediment respiration is relevant and important. We also acknowledge that a rigorous model-data comparison is desirable but not the year-to-year comparisons are hampered, to some degree, by the relatively limited availability of observational data. Observed rates of SOC are reported in the discussion. Also, we recently became aware of a nutrient data set for the region and have added the resulting comparisons to the new model validation section. Furthermore, we present model-data comparisons of satellite-derived SST and Chlorophyll, and model comparisons against in-situ data of temperature, salinity and oxygen. We believe that these comparisons provide the currently best attainable level of confidence in the model's ability for us to present model results. However, we fully agree that more would be much better. If the Reviewer is aware of any additional in-situ data that are available, we'd appreciate hearing about these and would happily include them.

With regard to the interannual variations shown in Figure 3: We have substantially expanded the analysis of these differences in the revised manuscript and sincerely hope the Reviewer finds it useful.

I would recommend to improve the model-data evaluation in order to convince that the modeling of hypoxia events are (1) not biased by model-dependent behaviors (2) close to observations.

Reply: We believe we have satisfactorily addressed both of these points. See responses to the comments about model drift and validation above.

Specific comments:

The model includes a light-attenuation term dependent on water depth and salinity (lines 177-181). Could you confirm that places where the light attenuation is applied ($f(z,S)$) are indeed places where particles (RDOM, Detritus , phytoplankton, . . .) are present and induce this shadowing effect ? Some other parameterisations exist that compute the shading directly in situ from the biogeochemical species. Using depth and salinity has the convenience to put this effect where it has been observed, but has the inconvenience to decouple the modeled biogeochemistry from its shading effect.

Reply: Thank you for raising this point. We have clarified that light is attenuated everywhere in the model domain by seawater constituents (specifically chlorophyll and detritus) and seawater itself. In addition to this, light is also attenuated by suspended sediment according to the parametrization referred to above. Observations show relatively higher suspended sediment concentrations, and thus light attenuation, in shallow areas (Bian et al., 2013; Chen et al., 2014). To account for this additional contribution to light attenuation by suspended sediment, which are not explicitly modeled, a simple parametrization depending on bathymetric depth and salinity is implemented. We is now clarified.

Minor comments

line 60. ref. Fennel & Testa : missing comma

line 187. "based on"

Figure 3 : labels a, b and c are missing on the figure itself.

Reply: We addressed these comments. Thank you for pointing them out.

Responses to Anonymous Referee #3

Below the review is reproduced in black font and our responses interspersed in blue.

Comments:

Summary: The manuscript introduces and shortly evaluates a new setup of a coupled physical-biogeochemical model of the East China Sea. With this model the authors show that the model reproduces observed hypoxic events and that it closely relates to the river discharge of the area, and present an oxygen budget that includes physical and biogeochemical processes.

Reply: We appreciate the Reviewer's overall positive assessment and believe we have addressed the concerns raised below as described.

Major comments: 1. The manuscript is overall well written and the figures are representative and easy to understand. However, as the manuscript is built at the moment, I lack a red thread and a consistent story in there. The manuscript starts by focusing on observed hypoxic events but it does not really go into details describing the processes behind, and why it looks different from year to year. Then the manuscript goes into describing the passage of typhoons and their effects on the oxygen concentrations, and after into describing oxygen budget for the area. This latter budget seem to be constructed by using simulated means over the whole simulation period (a description of how the budget is calculated is lacking). I would suggest that the authors focus on describing the hypoxic events, and that they dig more into the processes behind these to understand why it looks different from year to year. The authors see that the extent of hypoxic waters closely relates to the river discharge. However, they do not explain whether the increase in hypoxic waters is related to a stronger nutrient loading and thus an increase in the primary production and remineralization, or whether it is related to a stronger stratification preventing the exchange of oxygen between deep and surface waters. This could be analyzed by calculating a budget as the one that is presented in Figure 7 for each year. Further, it would be interesting if the authors could describe why they see a difference in the phenology of the hypoxic extent, and what causes the seasonal and interannual variations in the extent of CDW?

Reply: We have taken the Reviewer's suggestion to heart and substantially expanded the analysis of interannual and intra-seasonal variability. We agree that this was insufficiently developed in the previous version. We believe we now present a logical thread throughout the manuscript. The budget does not use simulated means but is calculated based on daily model output. Following the Reviewer's suggestion, we have included the individual years in the budget plot as well. The question whether variations in hypoxia are driven by freshwater variations (i.e. stratification = physical processes) or nutrient load variations (i.e. production & remineralization = biological processes) is now directly addressed. Interestingly, inputs of freshwater and nutrients are not correlated which allows us to separate the effects to some degree.

2. At the moment I do not see what your story gains with the section on typhoons. These processes are acting on much smaller time scales, and do not seem to have a large influence on the seasonal variations that you say that you will study in the abstract and in the introduction. I may be wrong, but in that case this should be clarified. If not I would suggest to remove this, or only briefly mention it and put the figure in the supplementary.

Reply: This is a fair point to raise and we agree that this point was not sufficiently developed. We have added a systematic analysis of high-wind events in the revised version. It turns out that the frequency of high-wind vents is important not only in explaining short-term variations but also interannual differences.

3. Are there more observations that you could use for your evaluation? Are there for example profiles of temperature/salinity/oxygen/nutrients measured during the hypoxic events that you present?

Reply: We don't have profile information (only surface and bottom concentrations for select properties) but fortunately we recently became aware of a suitable nutrient data set. We added a model-data comparison of nitrate distributions to the revised manuscript, which shows that the model does a good job in reproducing these.

Minor comments:

- the manuscript uses a lot of abbreviations that makes it difficult to follow. I would suggest to reduce them. You could remove abbreviations that are only used a few times, and keep those that are used all over the manuscript.

Reply: Agree. We are now limiting ourselves to a few acronyms that are repeated many times throughout the manuscript (ECS, CE, PP, OC, WOC, SOC and FW).

- use the word "evaluated" instead of "validated" all over the manuscript

Reply: The two words are not synonyms. Whenever we use the term "validated" we mean to do so.

- you need a section where you describe the observational data

Reply: We included a new section on model validation that also describes where the data come from.

- in the figures you have to specify what time-average you have plotted. Is it the modelled monthly means?

Reply: We don't show any monthly means. We added more explanation to the figure captions to make this clear and clarified in the text that we have saved daily output.

- page 1, line 16: replace "and reproduces" to "and it reproduces"

Reply: We prefer the sentence as is.

- in the introduction you could also add some examples from the Baltic Sea that also suffers from an increasing volume of low-oxygen waters.

Reply: The Baltic Sea is a very different system in that hypoxia and anoxia in its basins are essentially permanent. The hypoxic region in the ECS is in much shallower water, seasonal, and directly linked to the plume of a major river. The ECS is analogous to the northern Gulf of Mexico, and we draw comparisons between these two systems where appropriate throughout the manuscript, but we do not see the value in adding comparisons to the Baltic Sea.

-page 5. line 126: please specify how much 1/12 degree is in kilometres as these latitudes.

Reply: Done.

- page 5, line 128: do you have a reference for the MPDATA?

Reply: Yes, done.

- page 5, line 134: I guess the atmospheric forcing also contains solar radiation?

Reply: Yes, solar radiation is part of the heat fluxes (shortwave).

- page 5, line 137: describe in more detail what the SODA dataset contains, is it hourly, daily, weekly, monthly ... data?

Reply: Monthly, now added.

- page 5, line 144: please specify why you use daily river-runoff for this river and not the others. I guess it is because it is the major river in the area?

Reply: Yes, and because daily data are not available for the other rivers.

- Figure 1: what do the dots in the right hand panel show?

Reply: We changed this figure.

- page 7, line 173: is this instantaneous remineralization described in Laurent et al 2017? If not maybe you should describe it a bit more and why you have no burial in the sediments. What are the assumptions behind?

Reply: Yes, it is described in detail on Laurent et al. 2017 and also in Fennel et al. 2006.

- page 7, line 179: Maybe you could put a map in the supplementary material showing the attenuation coefficient? Does it compare well with observations (if there are any)?

Reply: We already have many figures in the Supplement and the attenuation coefficient moves with the river plume, so one static map wouldn't do much. No action taken.

- page 7, line 180: 1 year seems a bit short as spinup. Don't you have anymore drift C3 BGD
Interactive comment Printer-friendly version Discussion paper after this? What is the volume turnover time of the area?

Reply: On this point, please see the results from an 8-year climatological run we have conducted in response to comments by Reviewer 2. The plot included in the response shows that the model is in dynamics steady state in the region of interest after one year.

- page 7, what is the output frequency of diagnostics from the model?

Reply: We have daily output (and present daily concentrations and rates).

- page 10, line 223-225.

Reply: No action taken.

- Oxygen budget: you need to put some more details on how this is calculated. Is it calculated online or offline? If it is calculated offline, what output frequency do you use?

Reply: Physical terms are calculated online and written out daily and biological terms offline. We have stated in the model description that we use daily output.

- Page 14, line 282: You have not explained what the abbreviation WR stands for.

Reply: We have eliminated the abbreviation.

- Page 15, line 307: why is the turbulent diffusion stronger in the Northern region?

Reply: This text is gone.

- Page 16, line 341 and 348: Two sentences starting with "And". Sentences should not start with this word. Please reformulate.

Reply: This text is gone.

1 A numerical model study of the main factors contributing to
2 hypoxia and its interannual and intra-seasonal variability off the
3 Changjiang Estuary

4
5 Haiyan Zhang^{1,2}, Katja Fennel^{1,*}, Arnaud Laurent¹, Changwei Bian³

6
7 ¹Department of Oceanography, Dalhousie University, Halifax, Nova Scotia, Canada

8 ²School of Marine Science and Technology, Tianjin University, Tianjin, China

9 ³Physical Oceanography Laboratory/CIMST, Ocean University of China, and Qingdao
10 National Laboratory for Marine Science and Technology, Qingdao, China

11 *Corresponding author

12 **Abstract**

13 A three-dimensional physical-biological model of the marginal seas of China was used
14 to analyze interannual and intra-seasonal variations in hypoxic conditions and identify the
15 main processes controlling their generation off the Changjiang Estuary. The model was
16 validated against available observations and reproduces the observed temporal and spatial
17 variability of physical and biological properties including bottom oxygen. Interannual
18 variations of hypoxic extent are partly explained by variations in river discharge but not
19 nutrient load. The spatial extent of the freshwater plume is a useful metric when relating
20 riverine influences to biological rates and oxygen distributions. As riverine inputs of
21 freshwater and nutrients are consistently high, promoting large productivity and subsequent
22 oxygen consumption, wind forcing is important in modulating interannual and intra-
23 seasonal variability. Wind direction is relevant because it determines the spatial extent and
24 distribution of the freshwater plume which is strongly affected by either upwelling or
25 downwelling conditions. High-wind events can lead to partial reoxygenation of bottom
26 waters and, when occurring in succession throughout summer, can suppress the
27 development of hypoxic conditions. An oxygen budget is presented and shows that
28 sediment oxygen consumption is the dominant oxygen sink below the pycnocline, and that
29 advection of oxygen in the bottom waters acts as an oxygen sink in spring but becomes a

Deleted: sub-seasonal to

Deleted: of hypoxia

Deleted: Dissolved oxygen concentrations undergo a seasonal cycle, with minima generally occurring in August or September, and vary latitudinally with a longer duration of low-oxygen concentrations in the southern part of the hypoxic region.

Deleted: primarily associated with

Deleted: and wind forcing, with high river discharge promoting hypoxia generation. At synoptic time scales, strong wind events (e.g. typhoons) can disrupt hypoxic conditions. During the oxygen-depleted period (March-August), air-sea exchange acts as an oxygen sink in oversaturated surface waters. In the subsurface, biological oxygen consumption tends to dominate, but lateral physical transport of oxygen can be comparable during hypoxic conditions. Oxygen consumption in the water column exceeds that of the sediment when integrated over the whole water column, but ...

Deleted: . Vertical diffusion of oxygen acts as the primary oxygen source below the pycnocline and shows a seasonal cycle similar to that of primary production. A

52 source during hypoxic conditions in summer especially in the southern part of the hypoxic
53 region, which is influenced by open-ocean intrusions.

54

55 1. Introduction

56 In coastal seas, hypoxic conditions (oxygen concentrations lower than 2 mg L⁻¹ or 62.5
57 mmol m⁻³) are increasingly caused by rising anthropogenic nutrient loads from land (Diaz
58 & Rosenberg, 2008; Rabalais et al., 2010; Fennel and Testa, 2019). Hypoxic conditions are
59 detrimental to coastal ecosystems leading to a decrease in species diversity and rendering
60 these systems less resilient (Baird et al., 2004; Bishop et al., 2006; Wu, 2002). Hypoxia is
61 especially prevalent in coastal systems influenced by major rivers such as the northern Gulf
62 of Mexico (Bianchi et al., 2010), Chesapeake Bay (Li et al., 2016), and the Changjiang
63 Estuary (CE) in the East China Sea (Li et al., 2002).

64 The Changjiang River is the largest river in China and fifth largest in the world in terms
65 of volume transport, with an annual discharge of 9×10^{11} m³ year⁻¹ via its estuary (Liu et
66 al., 2003). The mouth of the CE is at the confluence of the southeastward Yellow Sea
67 Coastal Current and the northward Taiwan Warm Current (Figure 1). Hydrographic
68 properties in the outflow region of the CE are influenced by several different water masses
69 including fresh Changjiang Diluted Water, relatively low-salinity coastal water, more
70 saline water from the Taiwan Warm Current, and high-nutrient, low-oxygen water from
71 the subsurface of the Kuroshio (Wei et al., 2015; Yuan et al., 2008). The interactions of
72 these water masses together with wind forcing and tidal effects lead to a complicated and
73 dynamic environment.

74 Freshwater discharge reaches the minimum in winter when the strong northerly monsoon
75 (dry season) prevails and peaks in summer during the weak southerly monsoon (wet
76 season) resulting in a large freshwater (FW) plume adjacent to the estuary. Along with the
77 FW, the Changjiang River delivers large quantities of nutrients to the East China Sea (ECS)
78 resulting in eutrophication in the plume region (Li et al., 2014; Wang et al., 2016). Since
79 the 1970s, nutrient load has increased more than twofold with a subsequent increase in
80 primary production in the outflow region of the estuary (Liu et al., 2015). Hypoxia off the
81 CE was first detected in 1959 and, with a spatial extent of up to 15,000 km², is among the
82 largest coastal hypoxic zones in the world (Fennel & Testa, 2019). Although no conclusive

Deleted: TWC;

Deleted: (CDW)

Deleted: TWC

Deleted: river

Deleted: freshwater

Deleted: and the Yellow Sea (YS)

89 trend in oxygen minima has been observed (Wang, 2009; Zhu et al., 2011), hypoxic
90 conditions are suspected to have expanded and intensified in recent decades (Li et al., 2011;
91 Ning et al., 2011) due to the increasing nutrient loads from the Changjiang River (Liu et
92 al., 2015).

93 It is generally accepted that water-column stratification and the decomposition of
94 organic matter are the two essential factors for hypoxia generation, and this is also the case
95 for the shelf region off the CE (Chen et al., 2007; Li et al., 2002; Wei et al., 2007). High
96 solar radiation and freshwater input in summer contribute to strong vertical stratification
97 which is further enhanced by near-bottom advection of waters with high salinities (> 34)
98 and low temperatures (< 19 °C) ~~by the Taiwan Warm Current. The resulting~~ strong
99 stratification inhibits vertical oxygen supply (Li et al., 2002; Wang, 2009; Wei et al., 2007).
100 At the same time, high organic matter supply fuels microbial oxygen consumption in the
101 subsurface (Li et al., 2002; Wang, 2009; Wei et al., 2007; Zhu et al., 2011). It has also been
102 suggested that the TWC brings additional nutrients contributing to organic matter
103 production (Ning et al., 2011) and that the low oxygen concentrations (~ 5 mg L⁻¹) of the
104 TWC precondition the region to hypoxia (Ning et al., 2011; Wang, 2009).

105 While observational analyses suggest that hypoxia off the CE results from the interaction
106 of various physical and biogeochemical processes, quantifying the relative importance of
107 these processes and revealing the dynamic mechanisms underlying hypoxia development
108 and variability require numerical modeling (Peña et al., 2010). Numerical modeling studies
109 have proven useful for many other coastal hypoxic regions such as the Black Sea
110 northwestern shelf (Capet et al., 2013), Chesapeake Bay (Li et al., 2016; Scully, 2013), and
111 the northern Gulf of Mexico (Fennel et al., 2013; Laurent & Fennel, 2014).

112 Models have also been used to study the hypoxic region of the CE. Chen et al. (2015a)
113 used a 3D circulation model with a highly simplified oxygen consumption parameterization
114 (a constant consumption rate) to investigate the effects of physical processes, i.e.
115 freshwater discharge, and wind speed and direction, on hypoxia formation. Chen et al.
116 (2015b) examined the tidal modulation of hypoxia. The model domain in these two
117 previous studies was relatively limited encompassing only the CE, Hangzhou Bay and the
118 adjacent coastal ocean but did not cover the whole area affected by hypoxia (Wang, 2009;
119 Zhu et al., 2011). Zheng et al. (2016) employed a nitrogen cycle model coupled with a 3D

Deleted: TWC

Deleted: is

122 hydrodynamic model to examine the role of river discharge, wind speed and direction on
123 hypoxia, and also emphasized the physical controls. These previous modeling studies
124 focused on the response of hypoxia to physical factors only and did not address seasonal
125 evolution and interannual variations of hypoxia or the influence of variability in biological
126 rates.

127 More recently, Zhou et al. (2017) analyzed the seasonal evolution of hypoxia and the
128 importance of the Taiwan Warm Current and Kuroshio intrusions as a nutrient source using
129 an advanced coupled hydrodynamic-biological model. However, the baseline of their
130 model does not include sediment oxygen consumption (SOC), which is thought to be a
131 major oxygen sink in the hypoxic region off the CE (Zhang et al., 2017) and other river-
132 dominated hypoxic regions including the northern Gulf of Mexico (Fennel et al. 2013, Yu
133 et al. 2015a,b). Zhou et al. (2017) acknowledged the importance of SOC based on results
134 from a sensitivity experiment but did not quantify its role in hypoxia generation.

135 Here we introduce a new 3D physical-biological model implementation for the ECS that
136 explicitly includes nitrogen and phosphorus cycling and SOC. The model is a new regional
137 implementation for the ECS of an existing physical-biogeochemical model framework that
138 has been extensively used and validated for the northern Gulf of Mexico (Fennel et al.,
139 2011, 2013; Laurent et al., 2012; Laurent and Fennel, 2014; Yu et al., 2015b; Fennel and
140 Laurent, 2018). The hypoxic zones in northern Gulf of Mexico and off the CE have similar
141 features including the dominant influence of a major river (Changjiang and Mississippi), a
142 seasonal recurrence every summer, a typical maximum size of about 15,000 km²,
143 documented P-limitation following the major annual discharge in spring and a significant
144 contribution of SOC to oxygen sinks in the hypoxic zone (Fennel and Testa 2019). Here

145 the model is used to explore the evolution of hypoxia on interannual and intra-seasonal
146 scales and to identify the main factors contributing to the different modes of variability.
147 For this study, we performed and validated a 6-year simulation in the ECS, discuss the
148 main drivers of interannual and intra-seasonal variability, and present an oxygen budget to
149 quantify the relative importance of SOC and the influence of lateral advection of oxygen.

150 A companion study by Grosse et al. (2020) uses the same model to quantify the importance
151 of intrusions of nutrient-rich oceanic water from the Kuroshio for hypoxia development off
152 the CE.

Deleted: TWC

Deleted: subseasonal to

Deleted: short-term to

156 **2. Model description**

157 **2.1. Physical model**

158 The physical model used in this study is based on the Regional Ocean Modeling System
159 (ROMS; Haidvogel et al., 2008) and was implemented for the ECS by Bian et al. (2013a).
160 The model domain extends from 116°E to 134°E and from 20°N to 42°N (Figure 1),
161 covering the Bohai Sea, the Yellow Sea, the ECS, part of the Japan Sea and the adjacent
162 northwest Pacific, with a horizontal resolution of 1/12° (about 10 km) and 30 vertical layers
163 with enhanced resolution near the surface and bottom. The model uses the recursive
164 Multidimensional Positive Definite Advection Transport Algorithm (MPDATA) for the
165 advection of tracers (Smolarkiewicz and Margolin, 1998), a third-order upstream advection
166 of momentum, and the Generic Length Scale (GLS) turbulence closure scheme (Umlauf &
167 Burchard, 2003) for vertical mixing.

168 The model is initialized with climatological temperature and salinity from the World
169 Ocean Atlas 2013 V2 (WOA13 V2) (Locarnini et al., 2013; Zweng et al., 2013), and is
170 forced by 6-hourly wind stress, and heat and freshwater fluxes from the ECMWF ERA-
171 Interim dataset (Dee et al., 2011). Open boundary conditions for temperature and salinity
172 are prescribed from the monthly climatology (WOA13 V2), and horizontal velocities and
173 sea surface elevation at the boundaries are specified from the monthly SODA data set
174 (Carton & Giese, 2008). In addition, eight tidal constituents (M2, S2, N2, K2, K1, O1, P1
175 and Q1) are imposed based on tidal elevations and currents are extracted from the global
176 inverse tide model data set of TPXO7.2 of Oregon State University (OSU, Egbert &
177 Erofeeva, 2002). At the open boundaries, Chapman and Flather conditions are used for the
178 free surface and the barotropic velocity, respectively, and the radiation condition for the
179 baroclinic velocity. Eleven rivers are included in the model. Freshwater discharge from the
180 Changjiang River uses daily observations from the Datong Hydrological Station (DHS;
181 www.cjh.com.cn). Since daily observations are not available for the other rivers, we
182 prescribed monthly or annual climatologies (Liu et al., 2009; Tong et al., 2015; Zhang,
183 1996).

Deleted: ¶

Deleted: (BS)

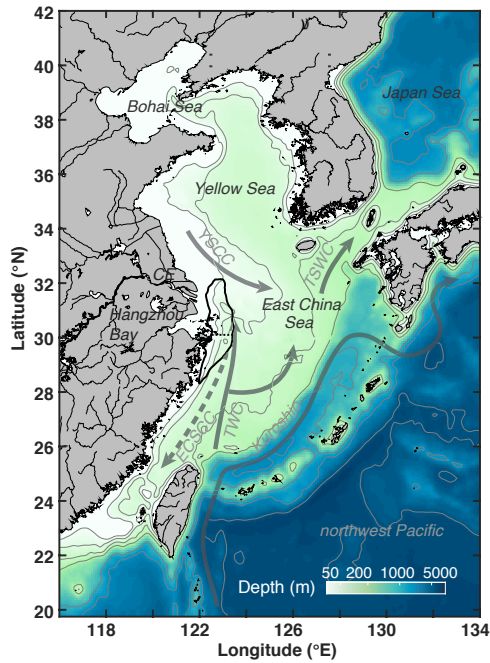
Deleted: S

Deleted: while

Deleted: are

Deleted: from

Deleted:



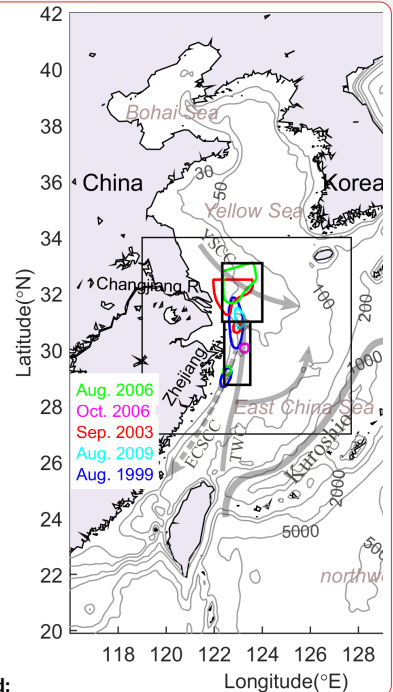
192

193 **Figure 1.** Bathymetry of the model domain with 30, 50, 100, 200, 1000, 2000 and 5000 m isobaths.
 194 The black outline near the Changjiang Estuary (CE) and Hangzhou Bay indicates the zone typically
 195 affected by low-oxygen conditions (dotted line shows separation between northern and southern
 196 zones). Solid grey arrows denote currents present throughout the year (Kuroshio; TWC: Taiwan
 197 Warm Current; YSCC: Yellow Sea Coastal Current). The dashed grey arrow indicates the direction
 198 of the wintertime East China Sea Coastal Current (ECSCC) which flows in the opposite direction
 199 to summertime flow.

200

201 **2.2. Biological model**

202 The biological component is based on the pelagic nitrogen cycle model of Fennel et al.
 203 (2006, 2011, 2013) and was extended to include phosphate (Laurent et al., 2012; Laurent
 204 & Fennel, 2014) and riverine dissolved organic matter (Yu et al., 2015b). The model
 205 includes two forms of dissolved inorganic nitrogen (DIN), nitrate (NO₃) and ammonium
 206 (NH₄), phosphate (PO₄), phytoplankton (Phy), chlorophyll (Chl), zooplankton (Zoo), two
 207 pools of detritus, suspended and slow-sinking small detritus (SDet) and fast-sinking large



Deleted:

Deleted: (left panel)

Deleted: (in meters)

Formatted: Not Highlight

Deleted: Colored polygons near the CE indicate observed hypoxic extent in previous studies (Li et al., 2002; Wei et al., 2007; Zhou et al., 2010; Zhu et al., 2016). Two small black boxes indicate the northern and southern regions used in the analysis. ...

Deleted: current

Deleted: here

Deleted: are

Deleted: in

Deleted: (ECSCC: East China Sea Coastal Current)

Deleted:

222 detritus (LDet), and riverine dissolved organic matter (RDOM). Here, riverine dissolved
223 and particulate organic nitrogen enter the pools of RDOM and SDet, respectively. The
224 remineralization rate of RDOM is an order of magnitude lower than that of SDet to account
225 for the more refractory nature of the riverine dissolved organic matter (Yu et al., 2015b).

226 At the sediment-water interface, SOC is parameterized assuming “instantaneous
227 remineralization,” i.e. all organic matter reaching the sediment is remineralized
228 instantaneously and oxygen is consumed due to nitrification and aerobic remineralization
229 at the same time. In the “instantaneous remineralization”, all phosphorus is returned to the
230 water column as PO₄ while a constant fraction of fixed nitrogen is lost due to denitrification.
231 All biogeochemical model parameters are given in Table S1 in the Supplement. A more
232 detailed model descriptions can be found in the Supplement to Laurent et al. (2017).

233 ~~Light is vertically attenuated by chlorophyll, detritus and seawater itself. In addition, to~~
234 ~~account for the effects of colored dissolved organic matter (CDOM) and suspended~~
235 ~~sediments, which show relatively high values near the coast and in the river plume (Bian~~
236 ~~et al., 2013b; Chen et al., 2014), a light-attenuation term dependent on water depth and~~
237 ~~salinity is introduced which yields higher attenuation in shallow areas and in the FW plume,~~

238 Initial and boundary conditions for NO₃, PO₄ and oxygen are prescribed using the
239 World Ocean Atlas 2013 (WOA13) climatology (Garcia et al., 2013a,b). A small positive
240 value is used for the other variables. NO₃ is nudged towards climatology in the northwest
241 Pacific at depth > 200 m. Monthly nutrient loads of NO₃ and PO₄ from the Changjiang are
242 from the Global-NEWs Model (Wang et al., 2015) but were adjusted by multiplicative
243 factors of 1.20 and 1.66, respectively, to ensure a match between simulated and observed
244 nutrient concentrations in the CE (see July and Aug 2012 in Figure 2). Nutrient loads in
245 other rivers are based other published climatologies (Liu et al., 2009; Tong et al., 2015;
246 Zhang, 1996).

247 We performed an 8-year simulation from 1 January 2006 to 31 December 2013, with
248 2006-2007 as model spin up and 2008-2013 used for analysis. ~~Model output was saved~~
249 ~~daily.~~

Deleted: T

Deleted: light attenuation due to

Deleted: er

Deleted: fresher areas

Deleted: DIN

Deleted: River

Deleted:

Deleted: Two geographical regions, the northern hypoxic region and the southern hypoxic region, are defined for analysis near the CE (Figure 1). The northern region corresponds to the Changjiang Bank and the southern region represents the submerged valley and Zhejiang coastal area.

3. Results

3.1. Model validation

The model is validated by comparing simulated surface and bottom temperature, salinity, current patterns and strengths, surface chlorophyll, surface nitrate and bottom oxygen to observations. The model reproduces remotely sensed spatial and temporal SST patterns (NOAA AVHRR; <https://www.nodc.noaa.gov/SatelliteData/ghrsst/>) very well with an annual correlation coefficient of 0.98 (Figure S1). Simulated surface and bottom salinity also show similar spatial and seasonal patterns as available *in situ* observations (Figures S2 and S3) with correlation coefficients of 0.77 and 0.84, respectively. Simulated surface and bottom temperature, when compared with available *in situ* data (Figures S4 and S5), are also consistent with the observations with correlation coefficients of 0.96 and 0.93.

The simulated current systems in the ECS and YS show typical seasonal variations as follows (see also Figure S6). In winter, currents mainly flow southward on the Yellow Sea and ECS shelves driven by the northerly wind. In contrast, the East China Sea Coastal Current and the Korean Coastal Current flow northward in summer. The Kuroshio is

Deleted: ¶

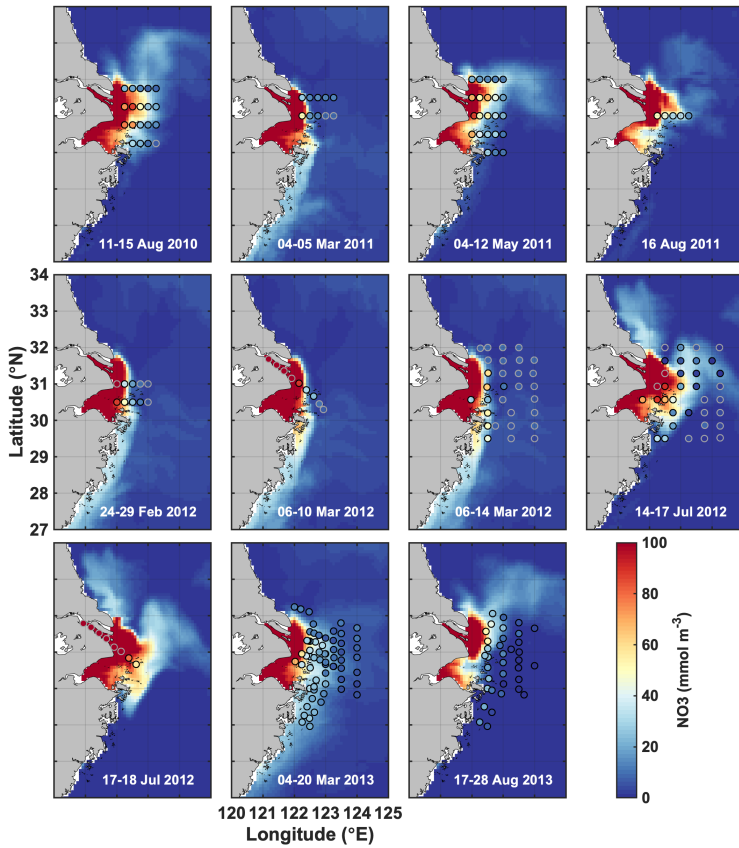


Figure 2: Simulated surface nitrate (colored map) shown for the day that marks the mid-point of the cruise dates (given in each panel) the compared to observations (dots) during 11 cruises from 2011 to 2013.

279 stronger in summer than in winter. The model captures the seasonal pattern of the current
 280 system and resolves currents in the ECS and Yellow Sea (also see Grosse et al. 2020).

281 Simulated monthly averaged (2008-2013) surface chlorophyll concentrations in May,
 282 August and November are compared with satellite-derived fields (MODIS-Terra;
 283 <http://oceancolor.gsfc.nasa.gov/>) and agree well with correlation coefficients of 0.77, 0.94
 284 and 0.64, respectively (Figure S7).

285 Simulated surface nitrate concentrations are shown in comparison to in situ observations
 286 in Figure 2 and agree well with a correlation coefficient of 0.84. Observations in March
 287 and July of 2012 show strongly elevated concentrations in the CE and a sharp gradient in
 288 the vicinity of the estuary's mouth that are well represented by the model. Likewise,
 289 simulated and observed bottom oxygen distributions are compared in Figure 3 and agree
 290 reasonably well overall with a correlation coefficient of 0.71, although the model
 291 underestimates observed low-oxygen conditions in July of 2011 and 2013 and August
 292 2013.

293 Together, these comparisons show that the model is able to reproduce important aspects
 294 of the physical-biogeochemical dynamics in the study region.

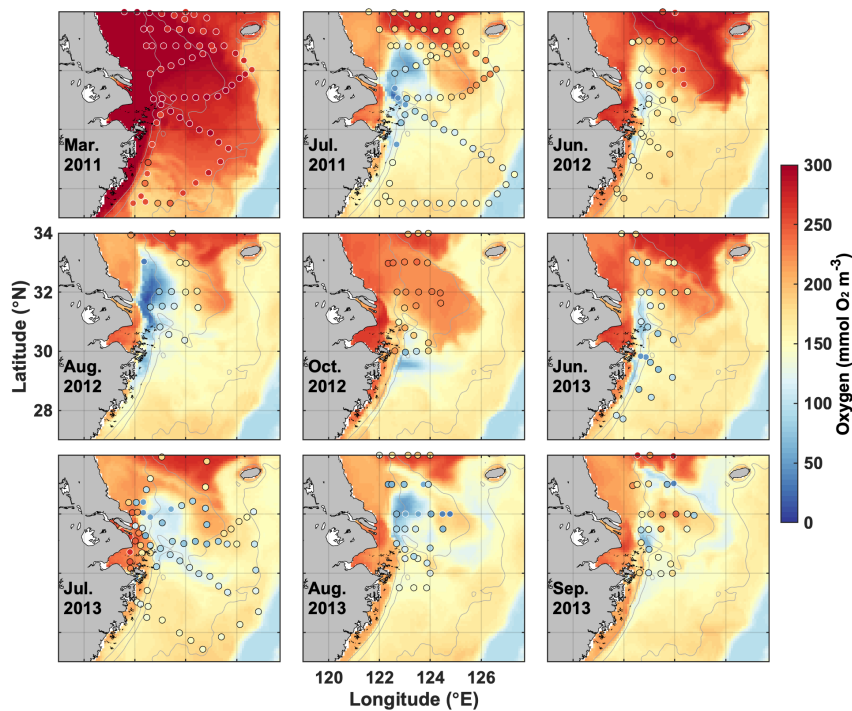


Figure 3. Simulated bottom oxygen (colored map) shown for the day that marks the mid-point of the cruise dates compared with observations (dots) during nine cruises from 2011 to 2013.

Deleted: First, we compare

Deleted: in near-bottom waters for 9 cruises between March 2011 and September 2013

Deleted: (

Deleted: 2)

Deleted: .

Deleted: T

Deleted: and observations agree well for the first 5 cruises in 2011 and 2012, but the simulated hypoxic area is smaller and less severe than

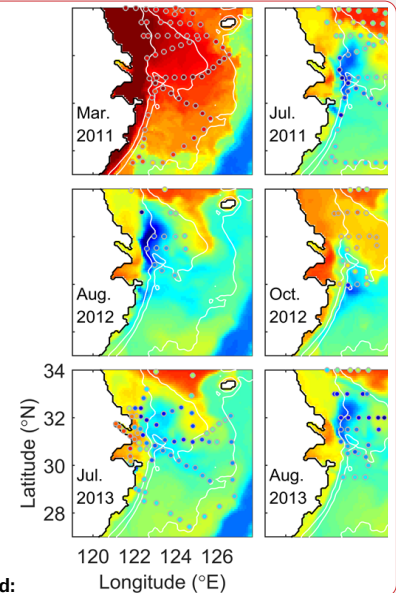
Deleted: June,

Deleted: Nevertheless, the model agrees well with the observed seasonal evolution and spatial distribution of observed bottom oxygen with an overall correlation coefficient of 0.76.

Deleted: Further validation of simulated surface and bottom distributions of temperature and salinity, a comparison of surface chlorophyll against satellite observations, and an assessment of the seasonal variations and transports of the major currents compared to observation-based estimates (H1)

Deleted: general and the spatio-temporal evolution of oxygen in bottom waters in particular

Deleted: .



Deleted:

Deleted: ¶

Deleted: 2

Formatted: Line spacing: 1.5 lines

3.2. Simulated oxygen dynamics

The model simulates annually recurring hypoxic conditions with a typical seasonal cycle where bottom waters are well-oxygenated until April/May, hypoxic conditions establish in June or July, become more pronounced in August, and disperse in October or November (Figure 4a, c). However, the model also simulates significant interannual variability in timing and extent of hypoxia over the 6-year simulation period (Figure 4b, c). The years with largest maximum hypoxic extent are 2010 (20,520 km²), 2009 (16,660 km²), 2012 (13,930 km²) and 2008 (12,720 km²) while the simulated hypoxic extent is much smaller (<5,000 km²) in 2011 and 2013. The ranking is similar when considering the time-integrated hypoxic extent (Figure 4b). The year with the largest maximum and integrated hypoxic extent (2010) also has the highest peak discharge (Figure 4a) and highest annual

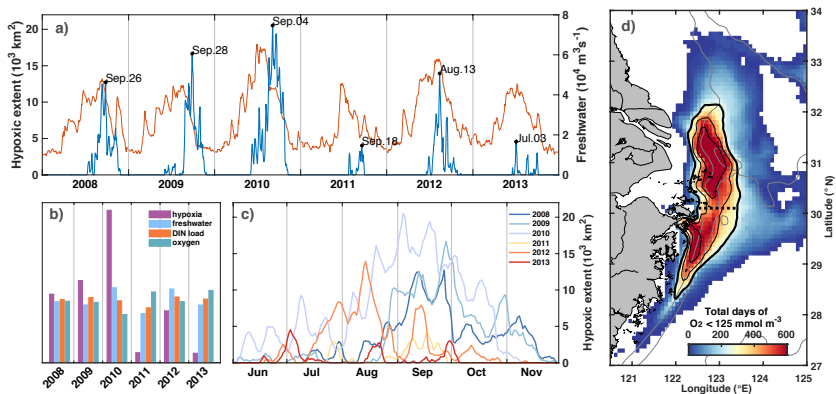


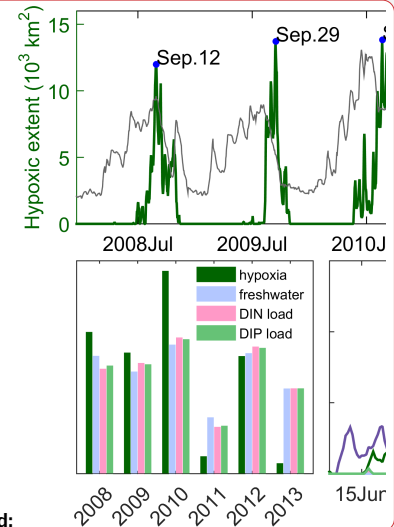
Figure 4. a) Time series of freshwater discharge and simulated hypoxic extent with peaks specified by date. b) Annual comparison of normalized time-integrated hypoxic extent, freshwater discharge, and DIN load, and summer-mean bottom oxygen concentration. c) Evolution of simulated hypoxic extent by year. d) Frequency map of number of days when bottom oxygen concentrations were below 125 mmol m⁻³ (4 mg/l). The black isolines indicate 240, 360 and 480 days (or 40, 60 and 80 days per year). The thick solid line indicates the region we refer to as the typical low-oxygen zone and the dashed line shows the demarcation between its northern and southern regions.

Deleted: In aggregate, ...he model simulates annually recurring hypoxic conditions with Figure 2 suggests ... typical seasonal cycle of hypoxia development...here with well-oxygenated ...ottom waters are well-oxygenated until April/Mayin March... hypoxic conditions establishing...in orand...July, becoming...morest...pronounced in August, and beginning to ...isperse in October or November (Figure 4a, c)September ... [2]

Moved (insertion) [1]

Deleted: Spatial distributions of bottom oxygen and surface salinity for the same year are shown in Figure 5 and illustrate their complex spatial patterns. Hypoxia appears first near the Zhejiang coast and further north in June and strengthens in July. In early August, hypoxia expands northward onto Changjiang Bank, while weakening and then disappearing near the Zhejiang coast. After reaching its peak extent on August 13, hypoxia starts to disperse in the northern regions and reappears further south near the Zhejiang coast in September. This spatial expression of hypoxia is mirrored in the spatial distribution of Changjiang Diluted Water (CDW), which generally extends southeastward or eastward in spring, veers northeastward in summer and then southeastward again in autumn relative to the mouth of the estuary (Figure 5). The patterns are similar in other years...owever, the model als[3]

Formatted: Line spacing: single



Deleted:

Deleted: 3... a) Time series of freshwater discharge and simulated hypoxic extent with peaks specified by date. b) Annual comparison of normalized time-integrated hypoxic extent, freshwater discharge, and DIN load, and summer-mean bottom oxygen concentration. c) Evolution of simulated hypoxic extent by year. d) Frequency map of number of days when bottom oxygen concentrations were below 125 mmol m⁻³ (4 mg/l). The blackb...isolines indicate 240, 360 and 480 days (or 40, 60 and 80 days per year). The thick solid line [4]

422 freshwater discharge ($65,400 \text{ m}^3 \text{ s}^{-1}$), although the annual discharge is similar to 2008 and
423 2012. ▾

424 The region where low-oxygen conditions are most commonly simulated is indicated by the
425 frequency map in Figure 4d, which shows the total number of days in the 6-year simulation
426 when bottom oxygen concentrations were below 125 mmol m^{-3} (or 4 mg/l), i.e. twice the
427 hypoxic threshold. It is known from observations that there are two centers of recurring
428 hypoxic conditions: the northern core is located just to the east of the CE and Hangzhou
429 Bay and the southern core to the southeast of Hangzhou Bay. The model is consistent with
430 these observations and simulates two distinct core regions of low-oxygen conditions
431 centered at 31°N and 29.3°N . The northern core region is larger than the southern core
432 region ($9,050 \text{ km}^2$ for a threshold of 80 days per year of $< 4 \text{ mg/l}$ compared to $5,230 \text{ km}^2$).
433 We will refer to the region defined by a threshold of 40 days of $< 4 \text{ mg/l}$ of per year (solid
434 black line in Figure 1 and 4d) as the “typical low-oxygen zone” for the remainder of the
435 manuscript and demarcate the northern and southern sections by 30.1°N latitude (dashed
436 line in Figures 1 and 4d).

437 There are marked differences in the phenology of simulated hypoxic extent (Figure 4c).
438 Among the four years with largest hypoxic areas, hypoxia establishes relatively late (mid-
439 August) and lasts long (into November) in 2008 and 2009. In contrast in 2012, hypoxic
440 conditions establish earlier (June), are most pronounced in August and are eroded by mid-
441 October. In 2010, the year with the largest peak extent, hypoxia establishes already at the
442 beginning of June and is maintained until the end of October, leading to the by far largest
443 time-integrated hypoxia among the 6 years (Figure 4b). In all years there are times when
444 hypoxic extent decreases rapidly. In the following sections we explore the drivers of
445 interannual and intra-seasonal variations in low-oxygen conditions and the role of
446 biological processes and physical forcing.

447 3.2.1 Interannual variations in hypoxia

448 As mentioned above, there is significant interannual variation in hypoxic extent in the 6-
449 year simulation (Figure 4a, b, c). The years with the largest time-integrated hypoxic events
450 are 2010, 2009 and 2008 followed by 2012 with the fourth largest hypoxic extent. In 2011
451 and 2013, hypoxic conditions were much less severe than in the other 4 years. Freshwater
452

Deleted: Since freshwater discharge and nutrient load are strongly related (Figure 3b), it is obvious that severe hypoxia is simulated in the years with large freshwater discharge and nutrient load.

Deleted: 3

Deleted: 3

Deleted: short periods

Deleted: during which the

461 (FW) input and nutrient load are less variable with the largest FW inputs in 2010 and 2012
 462 and the lowest in 2011. In an attempt to explain the interannual variations in hypoxia, we
 463 consider first the role of riverine FW inputs and nutrient loads. More specifically, we
 464 investigate correlations of time-integrated hypoxic area, average primary production (PP),
 465 total oxygen consumption (OC) by respiration, sediment oxygen consumption (SOC) and
 466 bottom oxygen in the typical low-oxygen zone, and the spatial extent of the FW plume with
 467 annually integrated FW input and DIN load (Figure 5).

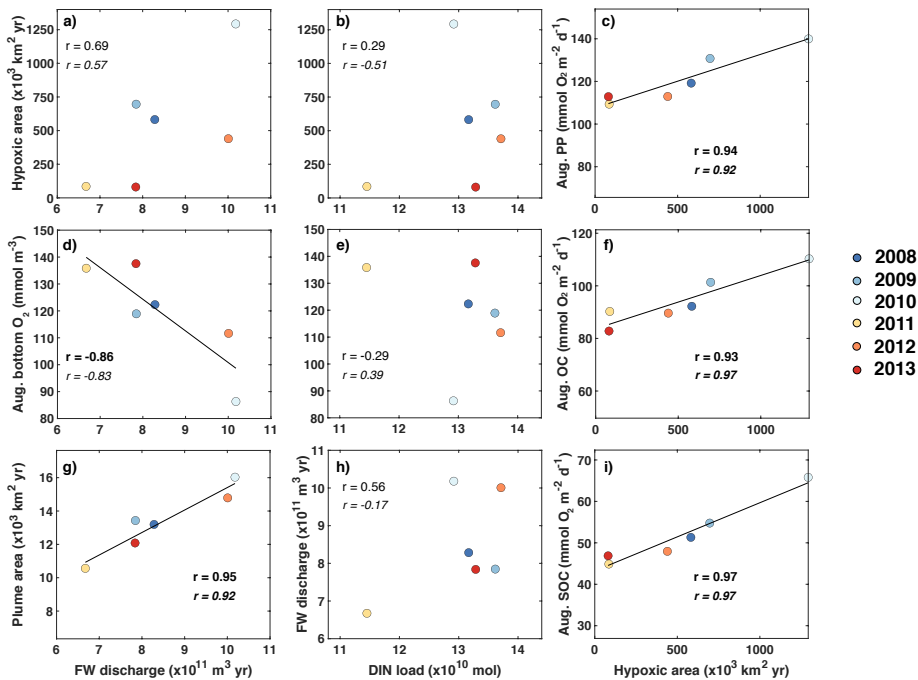


Figure 5. Correlations of time-integrated hypoxic area, average primary production, respiration and bottom oxygen in the typical low-oxygen zone in August, and the spatial extent of the FW plume (defined here as the area with surface salinity smaller than 25) with annually integrated FW input and DIN load. Correlation coefficients are given for all 6 years and, in italic font, after excluding year 2011. Significant correlations are shown in bold font and linear regressions indicated by the black line whenever the

468

469 There is a significant negative correlation between annual FW input and mean bottom-
470 water oxygen concentration in the low-oxygen zone of -86% and a weaker, statistically
471 insignificant positive correlation of 69% between annual FW input and integrated hypoxic
472 area (Figure 5a, d). This indicates that variations in FW input at least partly explain
473 variability in hypoxic conditions. Perhaps surprisingly, there is no convincing correlation
474 between annual FW input and annual DIN load (Figure 4h). Although the correlation
475 coefficient is 56% when all 6 years are considered, the correlation drops to -17% when the
476 low-flow year 2011 is excluded and neither of these correlations is statistically significant.
477 As expected, there is a strong positive correlation of 95% between annual FW input and
478 time-integrated plume area (Figure 4g). Plume area can thus be interpreted as a proxy of
479 FW input.

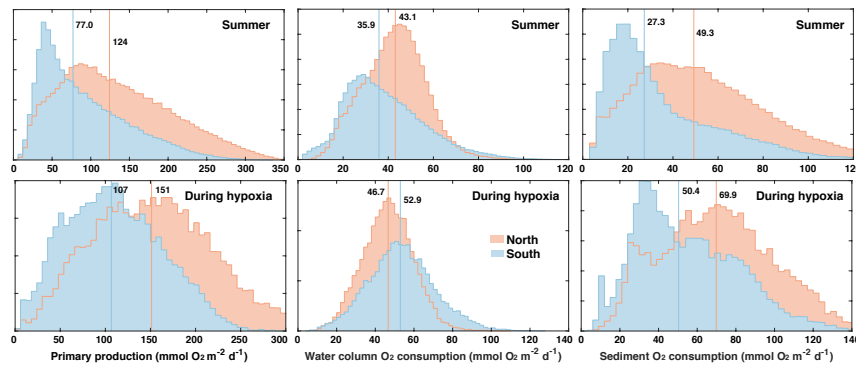
480 In contrast to the positive correlations between FW input and hypoxia as well as
481 bottom oxygen, correlations between the annual DIN load and integrated hypoxic area as
482 well as mean bottom-water oxygen are much weaker and insignificant (Figure 4b, e). This
483 implies that interannual variations in DIN load do not explain year-to-year variations in
484 hypoxia. However, the correlations between integrated hypoxic area and mean rates of PP
485 and OC (especially SOC) in August are significant and strong at 94% and 93% (97%),
486 respectively (Figure 5c, f, i). The high correlation between hypoxic area and OC is
487 primarily driven by SOC. Clearly, biological processes are important drivers of hypoxia
488 and contribute to its interannual variability, but they do not appear to result from variations
489 in DIN load. More relevant are variations in FW load, which explain interannual variations
490 in hypoxia at least partly.

491 Clearly, other factors than riverine inputs must be at play in driving interannual
492 variations. For example, comparing the years 2010 and 2012, both had very similar FW
493 input and DIN load, but differed in severity of hypoxia (Figure 5a, b). Likewise, the years
494 2009 and 2013 were very similar in terms of FW input and DIN load, but very different in
495 hypoxic extent. Next, we investigate the role of biological and physical drivers of intra-
496 seasonal and interannual variability in hypoxia.

497
498
499
500

501 **3.2.2 Biological drivers of intra-seasonal variability in hypoxia**

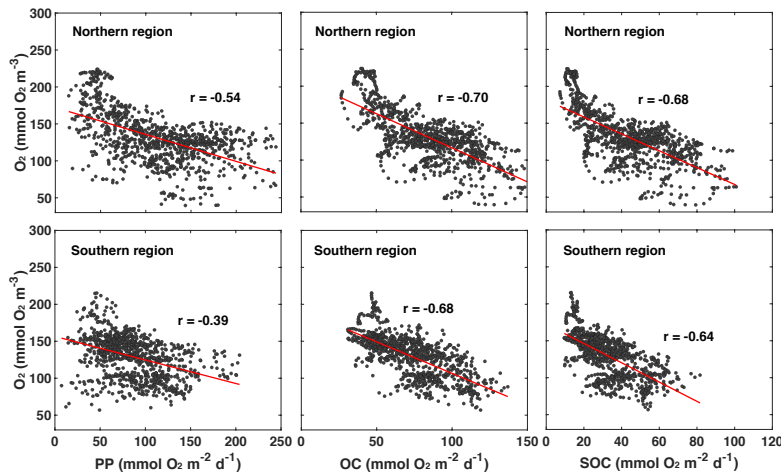
502 In order to explore whether biological rates are related to the presence of FW, and whether
503 the correlations that emerged when relating mean annual quantities also hold on shorter
504 time scales, it seems prudent to distinguish between the northern and southern regions. The
505 bathymetry in the northern zone is slightly deeper than in the southern zone (median depth
506 of 28.5 m versus 24.6 m) and several biological rates with direct relevance to oxygen
507 dynamics are different between the two zones (Figure 6). During the summer months (June
508 to September), primary production (PP), oxygen consumption in the water column
509 (WOC=OC-SOC), and SOC are larger in the northern zone with medians of 124 compared
510 to 77.0 mmol O₂ m⁻² d⁻¹ for PP, of 43.1 versus 35.9 mmol O₂ m⁻² d⁻¹ for WOC, and 49.3
511 versus 27.3 mmol O₂ m⁻² d⁻¹ for SOC. During hypoxic conditions, PP and SOC are also
512 notably larger in the northern zone with medians of 151 versus 107 mmol O₂ m⁻² d⁻¹ for PP
513 and 69.9 versus 50.4 mmol O₂ m⁻² d⁻¹ for SOC. In the water column, the difference is
514 reversed and WOC larger in the southern than the northern zone (52.9 versus 46.7 mmol
515 O₂ m⁻² d⁻¹). Because of these different characteristics, we consider the northern and
516 southern zones of the typical low-oxygen region separately.



517 **Figure 6:** Histograms primary production and water-column and sediment respiration during the
518 summer months (June to September) and during hypoxic conditions in the northern and southern
519 parts of the typically hypoxic zone. Medians are indicated by vertical lines.

521
522 The annual correlations presented in the previous section indicate that biological rates are
523 important drivers for interannual variability but not due to variations in nutrient load.

524 Variability in annual FW input is a better predictor. In order to better understand how
 525 variability in FW is related to biological rates and thus hypoxia, we first explore whether
 526 significant relationships exist between daily biological rates, bottom-water oxygen, and the
 527 presence of FW in the two zones. Since annual FW input is highly correlated with the
 528 extent of the FW plume (see Figure 5g), daily plume extent can be used as a measure of
 529 FW presence and compared to daily rates of PP, OC, SOC, and bottom oxygen.



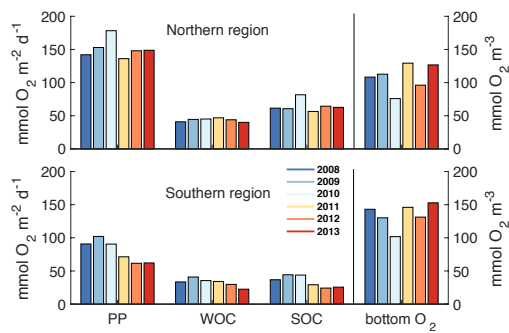
530 **Figure 7.** Correlations of daily averaged rates of PP, OC and SOC plotted with daily mean
 531 bottom oxygen concentration in the northern and southern regions of the low-oxygen zone in
 532 summer. The correlations are all significant. Correlation coefficients and slope and intercept of
 533 linear regressions (indicated by red lines) are given in Table 1.
 534

535

Relationships between bottom oxygen (mmol m^{-3}) in northern region and											
PP ($\text{mmol O}_2 \text{ m}^{-2} \text{ d}^{-1}$)			OC ($\text{mmol O}_2 \text{ m}^{-2} \text{ d}^{-1}$)			SOC ($\text{mmol O}_2 \text{ m}^{-2} \text{ d}^{-1}$)					
r	a	b	r	a	b	r	a	b			
-0.54	-0.36	172	-0.70	-0.92	209	-0.68	-1.14	181			
Same for the southern region											
-0.39	-0.32	157	-0.68	-0.85	192	-0.64	-1.30	172			
Relationships between plume area (10^3 km^2 ; defined by surface salinity < 29) in northern region and											
PP ($\text{mmol O}_2 \text{ m}^{-2} \text{ d}^{-1}$)			OC ($\text{mmol O}_2 \text{ m}^{-2} \text{ d}^{-1}$)			SOC ($\text{mmol O}_2 \text{ m}^{-2} \text{ d}^{-1}$)			Bottom oxygen (mmol m^{-3})		
0.62	6.04	47.6	0.49	2.48	57.7	0.51	2.05	22.0	-0.56	-3.74	171
Same for the southern region											
0.43	3.78	64.6	0.56	3.18	57.8	0.43	1.50	24.7	-0.49	-3.52	149

536 **Table 1.** Correlation coefficients and parameters of a linear model fit (of the form $y=ax+b$) between
 537

538 Daily PP, OC, and SOC are all significantly and negatively correlated with bottom-water
 539 oxygen (Figure 7, Table 1). This confirms that local production of organic matter and the
 540 resulting biological oxygen consumption are important for hypoxia development.
 541 However, it is also obvious that variability around the best fit is large (Figure 7).
 542 Furthermore, bottom oxygen and biological rates are significantly correlated with the
 543 extent of the FW plume (Table 1). This suggests that variability in the presence of FW
 544 contributes to variability in hypoxia not only by increasing vertical stratification and thus
 545 inhibiting vertical supply of oxygen to the subsurface but also because PP and respiration
 546 is larger in the river plume. Likely, large FW plumes stimulate more widespread biological
 547 production and thus oxygen consumption.



548
 549 **Figure 8.** Mean August rates of PP, WOC, and SOC and mean bottom oxygen concentration in the
 550 northern and southern regions for 6-year simulation.

551
 552 However, variations in biological rates alone do not explain variability in bottom
 553 oxygen concentrations and hypoxia. In Figure 8, we show August mean rates of PP, WOC,
 554 and SOC as well as mean bottom oxygen in the northern and southern zones for all years.
 555 In the northern zone, WOC is remarkably similar in all years. PP and SOC are also similar
 556 except in 2010 when SOC is higher. The low bottom oxygen concentration in 2010 could
 557 be explained by the relatively higher SOC; however, 2012 also had relatively low bottom
 558 oxygen while biological rates were similar to the other years with higher bottom oxygen.
 559 Likewise in the southern zone, differences in PP, WOC, and SOC among the years do not

560 explain differences in bottom oxygen, as the years with the lowest bottom oxygen (2010
561 and 2012) are not the years with the highest PP and oxygen consumption rates. Next, we
562 analyse the role of wind forcing, direction and stratification.

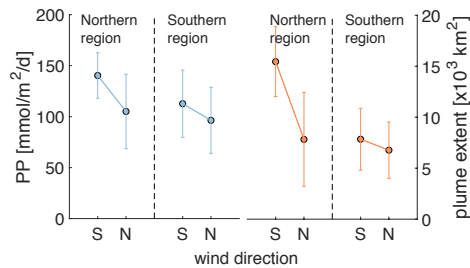
563

564 3.2.3 Physical drivers of intra-seasonal variability in hypoxia

565 We focus our analysis of physical drivers on wind direction and wind strength and
566 their relation to FW plume location and extent because the latter has already been identified
567 as an explanatory variable for interannual variations.

568 Wind direction is relevant because for most of June, July, and August winds blow
569 predominantly from the south, but switch to predominantly northerly winds between the
570 2nd half of August and the end of September. As a result of the northward, upwelling
571 favorable winds in the early summer, the FW plume is spread offshore and overlaps
572 primarily with the northern zone. After the switch to mostly southward, downwelling-
573 favorable directions, the FW plume moves southward, becomes more contained near the
574 coast, and grows in its southward extent as it is transported by a coastal current. Wind
575 direction has a demonstrable impact on PP and the extent of the FW plume as shown in
576 Figure 9 for the month of September. Especially in the region, PP and plume extent are
577 notably larger during southerly winds when the FW plume is more spread out, than during
578 northerly winds when the plume is restricted to the coastal current.

579



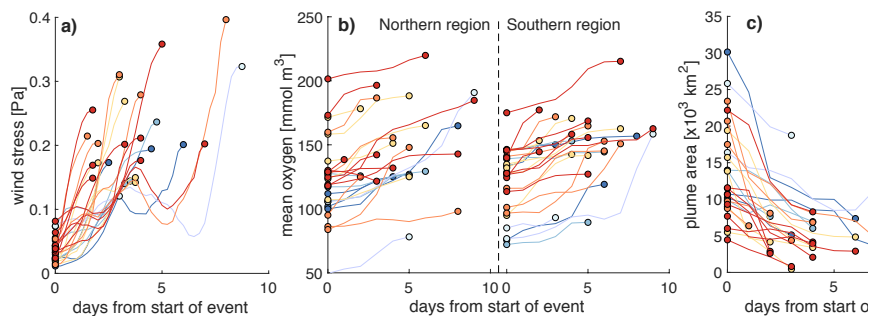
580

581 **Figure 9.** Mean PP and FW plume extent in the northern and southern regions averaged over days
582 with north and south wind (i.e. when direction is +/- 45° of true north or south) and wind strength
583 >0.03 Pa for in September.

584

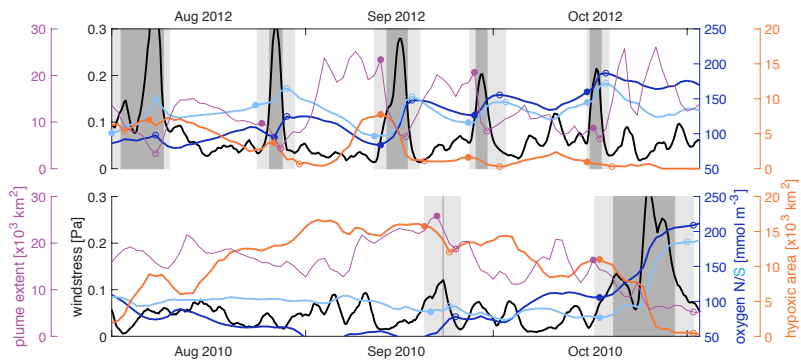
585 Wind strength is relevant because storm events can erode vertical stratification and
586 thus lead to resupply of oxygen to bottom waters due to vertical mixing. We investigated
587 the effect of wind strength on bottom oxygen, hypoxia, and the extent of the FW plume by
588 first inspecting time series of these variables (Figure S8). We isolated all event during the
589 months June to September and, in Figure 10, show the corresponding changes in wind
590 stress, mean bottom oxygen in the northern and southern zones, and the extent of the FW
591 plume. We diagnosed these events as follows. First, we identified all days when the wind
592 stress exceeded 0.12 Pa. Then we detected the minima in wind stress adjacent to the high-
593 wind days by searching for minima in wind stress within 3 days prior and 3 days after the
594 high-wind days. The periods within these minima are used as analysis period for each wind
595 event. In four instances the wind stress exceeded the threshold within 5 days of a previous
596 wind event. Those subsequent high-wind events were combined into one. We identified
597 the minimum in bottom oxygen (maximum in FW plume area) at the beginning of the event
598 and the maximum in oxygen (minimum in FW area) after the maximum in wind stress was
599 reached.

600 Figure 10a illustrates rapid increases in wind stress typically within 2 to 4 days. The
601 only exceptions are the 4 events where two storms occurred in rapid succession and the
602 combined event lasted longer (up to 8 days) until maximum wind stress was reached. The
603 year with the most wind events is 2013 (with 8 in total including one of the combined long-
604 lasting event). The year with the least events is 2010 (2 events) followed by 2009 (3 events).
605 Most of these events resulted in notable increases in mean bottom oxygen, typically by 10
606 to 30 mmol m⁻³, but up to 100 mmol m⁻³ in 2010 in the southern zone (Figure 10b). In the
607 rare cases where bottom oxygen did not increase or slightly decreased, bottom oxygen was
608 already elevated before the wind event. The wind events strongly affected the extent of the
609 FW plume (Figure 10c) by mixing the freshwater layer with underlying ocean water. The
610 effects are largest when the FW plume was most expansive. This analysis shows the
611 significant role of storm events in disrupting the generation of low-oxygen conditions and
612 ventilating bottom waters.



613
 614 **Figure 10.** Evolution of a) wind stress, b) bottom mean oxygen in the northern and southern
 615 regions, and c) extent of the FW plume during high-wind events. These events are defined by wind
 616 stress exceeding 0.12 Pa.

617
 618 In section 3.2.1 above, we noted that while the years 2010 and 2012 had very similar
 619 FW input and DIN load, 2010 had a much larger hypoxic area. Likewise, the years 2009
 620 and 2013 were very similar in terms of FW input and DIN load, but 2009 had a much larger
 621 hypoxic area. Considering the frequency and severity of high-wind events explains the
 622 differences in both cases.



623
 624 **Figure 11.** Wind stress (black), mean bottom oxygen in the northern and southern zones (dark and
 625 light blue), total hypoxic extent (orange), and FW plume extent (purple) throughout August,
 626 September and October of 2010 and 2012. The filled and open circles indicate a variables' value at

627 the beginning and after high-wind events. High-wind days/events are indicated by the dark/light
628 gray shading.

629 Figure 11 shows the wind stress, mean bottom oxygen in the northern and southern
630 zones, and total hypoxic extent and FW plume extent in 2012 and 2010. In 2012, there
631 were 5 high-wind events during the months of August, September, and October that all
632 coincided with increases in bottom oxygen, decreases in hypoxic extent when a hypoxic
633 zone was established at the beginning of the event, and decreases in FW plume extent.
634 Inspection of the evolution of bottom oxygen is especially instructive. While bottom
635 oxygen concentrations declined during periods with average or low wind, they were
636 essentially resented at a much higher level during each wind event. Whenever the FW plume
637 was extensive at the beginning of a high-wind event, it was drastically reduced during the
638 event. In 2010 bottom oxygen was at similar levels to 2012 at the beginning of August but
639 dropped to low levels throughout August, especially in the northern zone, and remained
640 low with widespread hypoxia until a major wind event in the second half of October
641 ventilated bottom waters. Except for a very short event in the second half of September,
642 there were no high-wind events from August until mid-October in 2010.

643 The differences in hypoxia in 2009 and 2013 can also be explained by the frequency
644 and intensity of high-wind events. In 2013, there were 8 high-wind events from July to
645 October that led to an almost continuous ventilation of bottom waters while in 2009 there
646 were only 3 such events during the same period (Figure S8). Low to average winds from
647 mid-August to early October of 2009 coincided with a decline in bottom oxygen and
648 establishment of an expansive hypoxic zone throughout most of September.

649 These analyses show that wind direction and strength play an important role in
650 determining the location of the hypoxic zone (i.e. northern versus southern region) and the
651 extent and severity of hypoxic conditions.

652 ▼ 653 **3.3 Oxygen budgets for the northern and southern regions**

654 In order to further investigate the roles of physical and biological processes in regulating
655 hypoxia, oxygen budgets are calculated from daily model output for the period from March
656 to August for the northern and southern hypoxic regions. Considering that hypoxic
657 conditions occur near the bottom, we evaluate an oxygen budget not only for the whole

Deleted: These decreases are due to wind events eroding vertical stratification and thus leading to resupply of oxygen over short time scales (days), as illustrated for 2012 in Figure 4. The year 2012 saw the passage of four typhoons (Haikui, Bolaven, Sanba and Prapiroon). Coincident with the passage of Haikui, Bolaven and Sanba (indicated by spikes in windstress), hypoxic area decreased, especially for Bolaven and Sanba. Prapiroon passed after hypoxia had eroded completely and thus had no effect (Figure 4a). Even moderate spikes in windstress (e.g., a week before Haikui and half-way between Sanba and Prapiroon) can lead to decreases in hypoxia extent. Panels 4b and c show that wind events lead to freshening of bottom water salinity, decreases in stratification strength (measured by N^2) and increases in bottom-water oxygen. However, not every decrease in hypoxic area is linked to a wind event; see, e.g., the slow decrease during the calm 2nd half of August where bottom salinity and stratification strength are decreasing and bottom-water oxygen increasing more slowly.¶

Deleted: 2

Deleted: identify

Deleted: key

Deleted: an

Deleted: is

682 water column but also for its lower portion ~~which~~ typically becomes hypoxic. To account
683 for variations in the thickness of the hypoxic layer, which tends to be thicker in deeper
684 waters (~~similar to~~ observations ~~by~~ Ning et al., 2011), we include the bottommost 12 layers
685 of our model grid. Because of the model's terrain-following vertical coordinates, the
686 thickness of these 12 model layers varies with total depth as shown. The terms considered
687 in the budget are air-sea flux, lateral physical advection and diffusion, vertical turbulent
688 diffusion (for the subsurface budget only), ~~PP~~, ~~WOC~~ (~~including~~ respiration and
689 nitrification), and SOC. Each term is integrated vertically over the whole water column and
690 also over the bottom-most 12 layers and then averaged for the northern and southern
691 regions for each month (Figure 12, Table S2).

Deleted: that

Deleted: also indicated by

Deleted: in

Deleted: by the gray lines in the oxygen panels in Figure 6

Deleted: photosynthetic production

Deleted: water-column oxygen consumption

Deleted: i.e.,

Deleted: 7

Deleted: in the Supplement

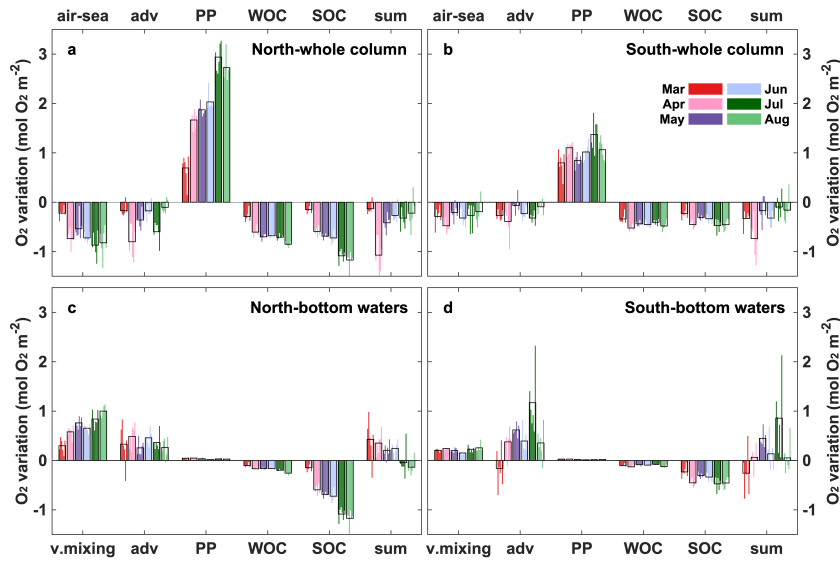
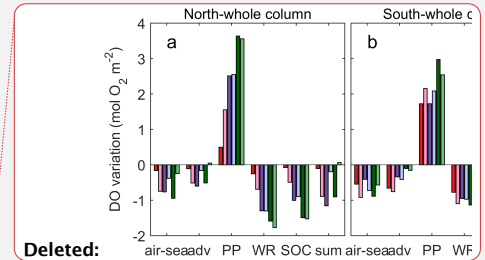


Figure 12. Monthly averaged (2008-2013) oxygen budgets for the whole water column and subsurface water from March to August in the northern and southern hypoxic regions. Adv represents lateral advection and lateral diffusion which is comparatively small, while v.mixing represents vertical turbulent diffusion, which is only relevant for the subsurface budget. Thin color bars represent individual years whereas the black bars are the 6-year average.



Deleted:

Deleted: 7

Deleted: (refer to Figure 1)

Deleted: (

Deleted:)

Deleted: . Diff

Deleted: 7

Deleted: R

Deleted: R

Deleted: -17% and 8%-27

Deleted: R

Deleted: R

Deleted: 54%-57% and 56%-58% in the northern and southern regions, respectively,

Deleted: SOC

Deleted: , which is

Deleted: associated with

Deleted: due to increasing temperature

Deleted: 7

Deleted: only 4%-

Deleted: 1

701 For the whole water column (Figure 12a, b), biological processes (PP, WOC, and SOC)
 702 greatly exceed physical processes (air-sea exchange and advective transport) in affecting
 703 oxygen. PP is always greater than the sum of WOC and SOC in the whole column
 704 indicating autotrophy in spring and summer. Advection is negative, acting as an oxygen
 705 sink and offsetting 21% of PP on average in the northern and southern regions. Of the two
 706 biological oxygen consumption terms (WOC and SOC), WOC accounts for half of total
 707 respiration. Negative air-sea flux indicates oxygen outgassing into the atmosphere and is
 708 due to photosynthetic oxygen production and decreasing oxygen solubility. However, since
 709 hypoxia only occurs in the subsurface, the subsurface budget below is more instructive.

710 When considering only subsurface waters (Figure 12c, d), the influence of PP decreases
 711 markedly, accounting for less than 2% of that in the whole water column. Vertical turbulent

727 diffusion acts as the largest oxygen source in the subsurface layer. SOC is the dominant
 728 oxygen sink accounting for 80% of the total biological oxygen consumption. As
 729 photosynthetic oxygen production increases gradually from spring to summer (Figure 12a,
 730 b) WOC, and SOC also increase as they are closely associated with photosynthetically
 731 produced organic matter. Vertical oxygen diffusion tends to covary with PP, implying an
 732 oxygen gradient driven by photosynthetic oxygen production in the upper layer. Lateral
 733 advection of oxygen is negative in March only (early in the hypoxic season) mainly in the
 734 southern region, but becomes positive later. This suggests that early in the hypoxic season,
 735 import of low-oxygen water contributes to hypoxia generation but advection switches to
 736 an oxygen source later. Overall, oxygen sources and sink terms are similar in the northern
 737 and southern regions.

738 ↓

739 **4. Discussion**

740 We implemented and validated a state-of-the-art physical-biological model for the ECS.
 741 The implementation is based on a model that was previously developed and extensively
 742 used for the northern Gulf of Mexico (Fennel et al. 2011, Laurent et al. 2012, Yu at
 743 al.2015b), a region that is similar to the ECS in that it receives large inputs of FW and
 744 nutrients from a major river and develops extensive, annually recurring hypoxia (see Table
 745 1 in Fennel and Testa (2019). Our model is more comprehensive than previous models for
 746 the ECS.

747 A 6-year simulation was performed and validated. The model faithfully represents
 748 patterns and variability in surface and bottom temperature and salinity, surface chlorophyll
 749 and nitrate distributions, bottom oxygen, and correctly simulates the major current patterns
 750 in the region (see Section 3.1 and Supplement). We thus deem the model's skill as
 751 sufficient for the analysis of biological and physical drivers of hypoxia generation
 752 presented here.

753 The model simulates annually recurring hypoxic conditions but with significant
 754 interannual and intra-seasonal variability and marked differences in phenology of hypoxic
 755 conditions from year to year (Figure 4a, b, c). Interannual variability in hypoxic conditions
 756 is much larger than variations in FW input, nutrient load, and bottom oxygen
 757 concentrations (Figure 4b) because small variations in oxygen can lead to large changes in

- Deleted: 1
- Deleted: -63% and 69%-73%
- Deleted: in the northern and southern regions, respectively
- Deleted: strengthens
- Deleted: see
- Deleted: 7
- Deleted: R
- Deleted: -
- Deleted: the
- Deleted: months of
- Deleted: (March, April
- Deleted: in both
- Deleted: s
- Deleted: (July, August) in the southern region
- Deleted: in both regions
- Deleted: in the southern region

Deleted: , except for turbulent diffusion from the upper layer into the subsurface which is much greater in the northern region

Moved up [1]: Spatial distributions of bottom oxygen and surface salinity for the same year are shown in Figure 5 and illustrate their complex spatial patterns. Hypoxia appears first near the Zhejiang coast and further north in June and strengthens in July. In early August, hypoxia expands northward onto Changjiang Bank, while weakening and then disappearing near the Zhejiang coast. After reaching its peak extent on August 13, hypoxia starts to disperse in the northern regions and reappears further south near the Zhejiang coast in September. This spatial expression of hypoxia is mirrored in the spatial distribution of Changjiang Diluted Water (CDW), which generally extends southeastward or eastward in spring, veers northeastward in summer and then southeastward again in autumn relative to the mouth of the estuary (Figure 5). The patterns are similar in other years.¶ Vertical distributions of temperature, salinity, oxygen and nutrients during hypoxic conditions are shown in Figure 6 to illustrate the spatial structure in the north-south, east-west and inshore-offshore directions. The north-south transect at 122.5°E shows relatively cold (< 20°C) and salty (> 34) bottom water with relatively high nitrate (> 5 µmol L⁻¹) and phosphate (~1 µmol L⁻¹) concentrations climbing inshore from the south and southeast. Bottom hypoxia occurs within this cold bottom water below the CDW (surface salinity < 28). The Yellow Sea Cold Water Mass (YSCWM), characterized by temperature less than 10°C, marks the northern boundary of hypoxic water. The cross-shore transects (32°N and PN) illustrate the offshore extension of the thin surface layer of CDW, its associated high nitrate concentrations, and the underlying hypoxic water. The

Deleted: Spatial distributions of bottom oxygen and surface salinity for the same year are shown in Figure 5 and illustrate

959 hypoxic area when bottom oxygen is near the hypoxic threshold. Interannual variability in
960 hypoxic area is partly explained by variations in annual FW input, consistent with previous
961 studies (Zheng et al., 2016; Zhou et al., 2017). While the correlation between time-
962 integrated hypoxic area and FW input is insignificant, there is a strong and significant
963 negative correlation between mean bottom oxygen in August and annual FW input (Figure
964 5). Annual FW input is also correlated strongly and significantly with the annually
965 integrated spatial extent of the FW plume, which is a useful metric for extent of the region
966 directly influenced by riverine inputs which induce strong density stratification and high
967 productivity.

968 Surprisingly, DIN load is not correlated with FW input, hypoxic area, and mean bottom
969 oxygen in August (Figure 5). This is in contrast to the northern Gulf of Mexico where DIN
970 load is highly correlated with both FW input and nutrient load and frequently used as a
971 predictor of hypoxic extent (Scavia et al. 2017, Laurent and Fennel 2019). However, the
972 lack of correlation between hypoxia and DIN load in the ECS should not be interpreted as
973 biological processes being unimportant in hypoxia generation, just that variations in DIN
974 load do not explain year-to-year differences. In fact, hypoxic area and biological rates (i.e.
975 mean August PP, OC, and SOC) are strongly and significantly correlated (Figure 5),
976 emphasizing the dominant role of biological oxygen consumption. The fact that riverine
977 variations in DIN load do not seem to have an effect suggests that riverine nutrient inputs
978 are large enough to saturate the region with nutrients, similar to the northern Gulf of
979 Mexico where small reductions in nutrient load have a relatively small effect (Fennel and
980 Laurent 2018).

981 Variations in riverine FW input only partly explain interannual variations in hypoxia.
982 For example, the years 2010 and 2012 had similar FW inputs and DIN loads but the hypoxic
983 area was 4 times larger in 2010 than 2012 (Figure 5a). Similarly, 2009 and 2013 had the
984 same FW inputs and nutrient loads but 2009 experienced extensive hypoxia while there
985 was almost none in 2013. In order to elucidate these differences, we investigated biological
986 and physical drivers of intra-seasonal variability.

987 In the ECS, two distinct zones of low oxygen have been observed (Li et al., 2002; Wei
988 et al., 2007; Zhu et al., 2016, 2011). The model simulates these two zones, referred to as
989 the northern and southern zone, consistent with observations (Figure 4d) and with generally

990 higher PP and SOC in the northern zone (Figure 6). Because of these differences we treated
991 the two zones separately in our analysis of intra-seasonal drivers.

992 We found daily biological rates (i.e. PP, OC, SOC) to be significantly correlated with
993 bottom oxygen in both zones, but with relatively large variability around the best linear fit
994 (Figure 7). The biological rates and bottom oxygen are also significantly correlated with
995 the extent of the FW plume (Table 1). Again, these results emphasize the dominant role of
996 biological oxygen consumption, and its relation to riverine inputs, in hypoxia generation
997 but leave a significant fraction of the variability unexplained.

998 We conducted an analysis of the effects of wind direction and strength on hypoxia. Wind
999 direction has a notable effect on the geographic distribution of hypoxia. Southerly,
1000 upwelling-favorable winds lead to a more widespread eastward extension of the FW plume
1001 with elevated PP and vertical density stratification (Figure 9). Northerly, downwelling-
1002 favorable winds create a coastally trapped southward jet that moves FW southward and
1003 constrains the plume close to the coast. A similar behavior has been described for the
1004 northern Gulf of Mexico (Feng et al. 2014).

1005 Wind strength turned out to be an important factor in hypoxia evolution. We identified
1006 high-wind events and showed that whenever bottom oxygen is low, a high-wind event will
1007 lead to a partial reoxygenation of bottom waters and decrease hypoxic extent (Figure 10).
1008 The impact of high-wind events is also visible in the extent of the FW plume, which is
1009 drastically reduced during high winds because FW is mixed. The frequency of high-wind
1010 events during summer explains the differences in hypoxic area between 2010 and 2012
1011 (Figure 11) and 2009 and 2013 (Figure S8). In 2009 and 2010 there were only few high-
1012 wind events during summer while 2012 and 2013 experienced a sequence of storms that
1013 led to partial reoxygenation of the water column throughout the summer and thus impeded
1014 the development hypoxia.

1015 We calculated oxygen budgets for the northern and southern regions considering the
1016 whole water-column and the near-bottom layer only. The subsurface budget is particularly
1017 useful in providing insights into when and where lateral advection amplifies or mitigates
1018 hypoxia and illustrates that SOC is the dominant oxygen sink in the subsurface. The relative
1019 importance of WOC and SOC had not previously been quantified for this region due to
1020 lack of concurrent WOC and SOC observations and lack of models that realistically

Formatted: First line: 0 ch

Deleted: The model simulates hypoxia in subsurface waters off the CE with two core centers: the southern region near the Zhejiang coast and in the submerged valley northeast of Zhejiang, and the northern region centered on Changjiang Bank. These model results are consistent with observed hypoxia locations (Li et al., 2002; Wei et al., 2007; Zhu et al., 2016, 2011). The simulated seasonal cycle of hypoxic conditions, developing first in the southern region, strengthening northward to reach their maximum extent between August and September, and then retreating southward, also agrees with the available observations (Wang et al., 2012; Zhu et al., 2011) albeit limited. The subseasonal north-south shifts in hypoxia location match shifts in the surface distribution of CDW, underscoring the important role of density stratification in facilitating hypoxic conditions. Relative to the CE mouth, the CDW generally extends southeastward in spring, veers northeastward to Cheju Island in summer and then again southeast in autumn, due to the Asian monsoon. The hypoxic layer is found below the main pycnocline and can be more than 20 m thick in August, in agreement with observations (Li et al., 2002; Ning et al., 2011).

Hypoxic extent exhibits pronounced interannual and subseasonal variability. Years with more severe hypoxia are also years with high river discharge and large associated nutrient loads, suggesting that these are the major factors controlling interannual variation of hypoxia off the CE. This is consistent with previous studies (Zheng et al., 2016; Zhou et al., 2017). In addition, the model simulates large variations in hypoxic extent on short time scales (days). Large and rapid decreases in hypoxic extent result from wind events, including typhoons, and can disrupt hypoxia multiple times throughout the same hypoxic season (as shown for 2012). Hypoxic conditions tend to be restored within a few days after typhoon passage; a phenomenon that has been documented by time series observations in the region (Ni et al., 2016; Wang et al. 2017).

Oxygen budgets for the northern and southern regions typically encompassing the hypoxic zones provide valuable insights into the importance of surface and subsurface processes, the dominant role of SOC in the subsurface and the contribution of horizontal advection of oxygen to regional and seasonal hypoxia dynamics. When considering the whole water column, which is always autotrophic in these regions, biological processes greatly exceed lateral transport of oxygen. Lateral oxygen transport always acts as a sink. And WR accounts for more than half of the biological oxygen. [6]

Deleted: is

Deleted: comparison between whole-water column and

Deleted: -only

Deleted: s emphasizes the importance of considering the latter, ...

Deleted: ing

Deleted: that

Deleted: R

Deleted: R

Deleted:

Deleted: observed

Deleted: 14.3

Deleted: 15.4

Deleted: R

1136 account for both processes. The budget for the whole water column is less useful because
1137 it is dominated by the oxygen sources, sinks and transport in the surface layer, which does
1138 not experience hypoxia and thus is not relevant.

1139 The importance of SOC in our model is consistent with recent observational studies in
1140 the ECS. SOC on the coastal shelves in the Yellow Sea and ECS has been estimated to
1141 range from 1.7 to 17.6 mmol O₂ m⁻² d⁻¹ (mean rate of 7.2 mmol O₂ m⁻² d⁻¹) from April to
1142 October except August by Song et al. (2016), and from 9.1 to 62.5 mmol O₂ m⁻² d⁻¹ (mean
1143 of 22.6 ± 16.4 mmol O₂ m⁻² d⁻¹) from June to October in Zhang et al. (2017). Simulated
1144 SOC in the typical low-oxygen zone falls within the range observed by Zhang et al. (2017)
1145 with a mean rate of 20.6 ± 19.2 mmol O₂ m⁻² d⁻¹ between April and October. Based on
1146 observations, Zhang et al. (2017) already suggested that SOC is a major contributor to
1147 hypoxia formation in below-pycnocline waters, which is further corroborated by our model
1148 results. It is also consistent with the modelling study of Zhou et al. (2017), who did not
1149 include SOC in the baseline version of their model but showed in a sensitivity study that
1150 inclusion of SOC simulates hypoxic extent more realistically. Our results are in line with
1151 findings from the northern Gulf of Mexico hypoxic zone where WOC_v is much larger than
1152 SOC below the pycnocline, while SOC is dominant in the bottom 5 m where hypoxia
1153 occurs most frequently in summer (Quiñones-Rivera et al., 2007; Yu et al., 2015b).

1154 The finding that lateral oxygen transport can act as a net source to subsurface water is
1155 also new. On seasonal scales, oxygen advection in the subsurface varies from an oxygen
1156 sink in spring to a source in summer, especially in the southern hypoxic region, implying
1157 that the TWC becomes an oxygen source when oxygen is depleted in the hypoxic region.
1158 This aspect was neglected in previous studies which only emphasized the role of advection
1159 as an oxygen sink promoting hypoxia formation (Ning et al., 2011; Qian et al., 2015). The
1160 TWC originates from the subsurface of the Kuroshio northeast to Taiwan Island, and thus
1161 represents an intrusion onto the continental shelves from the open ocean (Guo et al., 2006).
1162 In addition to oxygen advection, nutrients are transported supporting primary production
1163 on the ECS shelves (Zhao & Guo, 2011, Grosse et al. 2020). The intrusion of the TWC and
1164 the Kuroshio accompanied by relatively cold and saline water, and nutrient and oxygen
1165 transport, is thought to influence hypoxia development (Li et al., 2002; Wang, 2009; Zhou

1171 et al., 2017) but no quantification of the relative importance has occurred until now (see
1172 companion paper by Grosse et al., 2020, using the same model).

Deleted:

1174 5. Conclusions

1175 In this study, a new 3D coupled physical-biological model for the ECS was presented
1176 and used to explore the spatial and temporal evolution of hypoxia off the CE and to quantify
1177 the major processes controlling interannual and intra-seasonal oxygen dynamics.
1178 Validation shows that the model reproduces the observed spatial distribution and temporal
1179 evolution of physical and biological variables well.

Deleted: Overall, simulated hypoxia generally occurs near the Zhejiang coast and the submerged valley to its east (the southern hypoxic region) and on the Changjiang Bank (the northern region) and is dominated by behavior of the CDW and local wind-driven current system. Simulated hypoxia duration is generally longer in the southern hypoxic region.

1180 A 6-year simulation with realistic forcing produced large interannual and intra-seasonal
1181 variability in hypoxic extent despite relatively modest variations in FW input and nutrient
1182 loads. The interannual variations are partly explained by variations in FW input but not
1183 DIN load. Nevertheless, elevated rates of biological oxygen consumption are of paramount
1184 importance for hypoxia generation in this region, as shown by the high correlation between
1185 hypoxic area, bottom oxygen, and biological rates (PP, OC, SOC) on both annual and
1186 shorter time scales.

1187 Other important explanatory variables of variability in hypoxia are wind direction and
1188 strength. Wind direction affects the magnitude of PP and the spatial extent of the FW plume,
1189 because southerly, upwelling favorable winds tend to spread the plume over a large area
1190 while northerly, downwelling-favorable winds push the plume against the coast and induce
1191 a coastal current the contains the FW and moves it downcoast. Wind strength is important
1192 because high-wind events lead to a partial reoxygenation whenever bottom oxygen is low
1193 and can dramatically decrease the extent of the FW plume. The frequency of high-wind
1194 events explains some of the interannual differences in hypoxia, where years with similar
1195 FW input, nutrient load, and mean rates of oxygen consumption have display very different
1196 hypoxic extents because high-wind events lead to partial reoxygenation of bottom waters.

Deleted: Pronounced interannual variations of hypoxic extent in our 6-year simulation are primarily associated with differences in river discharge and nutrient load as larger freshwater and nutrient inputs enhance water column stratification and primary production, respectively, and thus are conducive to hypoxia development. On synoptic time scales, strong wind events (e.g. typhoons) can disrupt simulated hypoxia significantly, but only for short periods.

1197 A model-derived oxygen budget shows that SOC is larger than WOC in the subsurface
1198 of the hypoxic region. Lateral advection of oxygen in the subsurface switches from an
1199 oxygen sink in spring to a source in summer especially in the southern region and is likely
1200 associated with open-ocean intrusions onto the coastal shelf supplied by the Taiwan Warm
1201 Current.

Deleted: R

Deleted: oxygen

Deleted: hypoxic

Deleted: the TWC supplying

1221

1222 **Acknowledgments**

1223 This work was supported by the National Key Research and Development Program of
1224 China (2016YFC1401602 and 2017YFC1404403). The authors thank the crew of the
1225 Dongfanghong2 for providing much help during the sampling cruises, and Compute
1226 Canada for access to supercomputer time. Financial support to HZ from the China
1227 Scholarship Council (CSC) is gratefully acknowledged. KF also acknowledges support
1228 from the NSERC Discovery Program. The model forcing datasets (WOA, ECMWF, SODA,
1229 TPXO7.2) used in this study are publicly available and related papers are cited in the
1230 reference list. Websites of the satellite data (SST, chlorophyll) and the Changjiang
1231 freshwater data have been given where they are used. Nutrients data of rivers are available
1232 in published papers cited in the reference list. The model results are available on request to
1233 the authors.

1234

1235 **References**

- 1236 Baird, D., Christian, R. R., Peterson, C. H., & Johnson, G. A.: Consequences of hypoxia on
1237 estuarine ecosystem function: Energy diversion from consumers to microbes. *Ecological*
1238 *Applications*, 14(3), 805–822. <https://doi.org/10.1890/02-5094>, 2004.
- 1239 Bian, C., Jiang, W., & Greatbatch, R. J.: An exploratory model study of sediment transport
1240 sources and deposits in the Bohai Sea, Yellow Sea, and East China Sea. *Journal of Geophysical*
1241 *Research: Oceans*, 118(11), 5908–5923. <https://doi.org/10.1002/2013JC009116>, 2013a.
- 1242 Bian, C., Jiang, W., Quan, Q., Wang, T., Greatbatch, R. J., & Li, W.: Distributions of suspended
1243 sediment concentration in the Yellow Sea and the East China Sea based on field surveys during
1244 the four seasons of 2011. *Journal of Marine Systems*, 121–122, 24–35,
1245 <https://doi.org/10.1016/j.jmarsys.2013.03.013>, 2013b.
- 1246 Bianchi, T. S., DiMarco, S. F., Cowan, J. H., Hetland, R. D., Chapman, P., Day, J. W., & Allison,
1247 M. A.: The science of hypoxia in the northern Gulf of Mexico: A review. *Science of the Total*
1248 *Environment*, 408(7), 1471–1484. <https://doi.org/10.1016/j.scitotenv.2009.11.047>, 2010.
- 1249 Bishop, M. J., Powers, S. P., Porter, H. J., & Peterson, C. H.: Benthic biological effects of
1250 seasonal hypoxia in a eutrophic estuary predate rapid coastal development. *Estuarine, Coastal*
1251 *and Shelf Science*, 70(3), 415–422. <https://doi.org/10.1016/j.ecss.2006.06.031>, 2006.
- 1252 Capet, A., Beckers, J. M., & Grégoire, M.: Drivers, mechanisms and long-term variability of
1253 seasonal hypoxia on the Black Sea northwestern shelf - Is there any recovery after

1254 eutrophication? *Biogeosciences*, 10(6), 3943–3962. <https://doi.org/10.5194/bg-10-3943-2013>,
1255 2013.

1256 Carton, J. A., & Giese, B. S.: A Reanalysis of Ocean Climate Using Simple Ocean Data
1257 Assimilation (SODA). *Monthly Weather Review*, 136(8), 2999–3017,
1258 <https://doi.org/10.1175/2007MWR1978.1>, 2008.

1259 Chen, C. C., Gong, G. C., & Shiah, F. K., Hypoxia in the East China Sea: One of the largest
1260 coastal low-oxygen areas in the world. *Marine Environmental Research*, 64(4), 399–408.
1261 <https://doi.org/10.1016/j.marenvres.2007.01.007>, 2007.

1262 Chen, J., Cui, T., Ishizaka, J., & Lin, C.: A neural network model for remote sensing of diffuse
1263 attenuation coefficient in global oceanic and coastal waters: Exemplifying the applicability of
1264 the model to the coastal regions in Eastern China Seas. *Remote Sensing of Environment*, 148,
1265 168–177. <https://doi.org/10.1016/j.rse.2014.02.019>, 2014.

1266 Chen, X., Shen, Z., Li, Y., & Yang, Y.: Physical controls of hypoxia in waters adjacent to the
1267 Yangtze Estuary: A numerical modeling study. *Marine Pollution Bulletin*, 97(1–2), 349–364.
1268 <https://doi.org/10.1016/j.marpolbul.2015.05.067>, 2015a.

1269 Chen, X., Shen, Z., Li, Y., & Yang, Y.: Tidal modulation of the hypoxia adjacent to the Yangtze
1270 Estuary in summer. *Marine Pollution Bulletin*, 100(1), 453–463,
1271 <https://doi.org/10.1016/j.marpolbul.2015.08.005>, 2015b.

1272 Dee, D. P., Uppala, S. M., Simmons, A. J., Berrisford, P., Poli, P., Kobayashi, S., ... Vitart, F.:
1273 The ERA-Interim reanalysis: Configuration and performance of the data assimilation system.
1274 *Quarterly Journal of the Royal Meteorological Society*, 137(656), 553–597.
1275 <https://doi.org/10.1002/qj.828>, 2011.

1276 Diaz, R. J., & Rosenberg, R.: Spreading dead zones and consequences for marine ecosystems.
1277 *Science*, 321(5891), 926–929. <https://doi.org/10.1126/science.1156401>, 2008.

1278 Egbert, G. D., & Erofeeva, S. Y.: Efficient inverse modeling of barotropic ocean tides. *Journal of*
1279 *Atmospheric and Oceanic Technology*, 19(2), 183–204. [https://doi.org/10.1175/1520-0426\(2002\)019<0183:EIMOBO>2.0.CO;2](https://doi.org/10.1175/1520-0426(2002)019<0183:EIMOBO>2.0.CO;2), 2002.

1280 [Feng, Y., Fennel, K., Jackson, G.A., DiMarco, S.F. & Hetland, R.D.: A model study of the](#)
1281 [response of hypoxia to upwelling favorable wind on the northern Gulf of Mexico shelf, *Journal*](#)
1282 [of Marine Systems](#) 131, 63-73, 2014.

1283
1284 Fennel, K., and Testa, J.M.: Biogeochemical controls on coastal hypoxia, *Annual Review of*
1285 *Marine Science*, 11, 105-130, <https://doi.org/10.1146/annurev-marine-010318-095138>, 2019.

1286 Fennel, K. and Laurent, A.: N and P as ultimate and proximate limiting nutrients in the northern
1287 Gulf of Mexico: implications for hypoxia reduction strategies, *Biogeosciences*, 15, 3121-3131,
1288 <https://doi.org/10.5194/bg-15-3121-2018>, 2018.

1289 Fennel, K., Hetland, R., Feng, Y., & DiMarco, S.: A coupled physical-biological model of the
1290 Northern Gulf of Mexico shelf: Model description, validation and analysis of phytoplankton
1291 variability. *Biogeosciences*, 8(7), 1881–1899. <https://doi.org/10.5194/bg-8-1881-2011>, 2011.

1292 Fennel, K., Hu, J., Laurent, A., Marta-Almeida, M., & Hetland, R.: Sensitivity of hypoxia
1293 predictions for the northern Gulf of Mexico to sediment oxygen consumption and model
1294 nesting. *Journal of Geophysical Research: Oceans*, 118(2), 990–1002.
1295 <https://doi.org/10.1002/jgrc.20077>, 2013.

1296 Fennel, K., Wilkin, J., Levin, J., Moisan, J., O'Reilly, J., & Haidvogel, D.: Nitrogen cycling in
1297 the Middle Atlantic Bight: Results from a three-dimensional model and implications for the
1298 North Atlantic nitrogen budget. *Global Biogeochemical Cycles*, 20(3), 1–14.
1299 <https://doi.org/10.1029/2005GB002456>, 2006.

1300 Garcia, H. E., Boyer, T. P., Locarnini, R. A., Antonov, J. I., Mishonov, A. V., Baranova, O. K., ...
1301 Johnson, D. R.: World Ocean Atlas 2013. Volume 3: dissolved oxygen, apparent oxygen
1302 utilization, and oxygen saturation. NOAA Atlas NESDIS 75, 2013a.

1303 Garcia, H. E., Locarnini, R. A., Boyer, T. P., Antonov, J. I., Baranova, O. K., Zweng, M. M., ...
1304 Johnson, D. R.: World Ocean Atlas 2013, Volume 4 : Dissolved Inorganic Nutrients
1305 (phosphate, nitrate, silicate). NOAA Atlas NESDIS 76 (Vol. 4), 2013b.

1306 Grosse, F., Fennel, K., Zhang, H., Laurent, A.: Quantifying the contributions of riverine vs.
1307 oceanic nitrogen to hypoxia in the East China Sea, *Biogeosciences*, [https://doi.org/10.5194/bg-](https://doi.org/10.5194/bg-2019-342)
1308 [2019-342](https://doi.org/10.5194/bg-2019-342), **accepted for publication**.

1309 Guo, J. S., X. M. Hu and Y. L. Yuan: A diagnostic analysis of variations in volume transport
1310 through the Taiwan Strait using satellite altimeter data, *Advances in Marine Science*, 23(1):
1311 20 - 26 (in Chinese with English abstract), 2005.

1312 Haidvogel, D. B., Arango, H., Budgell, W. P., Cornuelle, B. D., Curchitser, E., Di Lorenzo, E., ...
1313 Wilkin, J., Ocean forecasting in terrain-following coordinates: Formulation and skill
1314 assessment of the Regional Ocean Modeling System. *Journal of Computational Physics*,
1315 227(7), 3595–3624. <https://doi.org/10.1016/j.jcp.2007.06.016>, 2008.

1316 Laurent, A., & Fennel, K.: Simulated reduction of hypoxia in the northern Gulf of Mexico due to
1317 phosphorus limitation. *Elementa: Science of the Anthropocene*, 2(1), 000022.
1318 <https://doi.org/10.12952/journal.elementa.000022>, 2014.

Deleted: (submitted to same

Deleted: Special Issue; ms bg-2019-342)

- 1321 [Laurent, A., Fennel, K.: Time-evolving, spatially explicit forecasts of the northern Gulf of](#)
1322 [Mexico hypoxic zone. *Environmental Science & Technology*, 53, 14,449-14,458, doi:](#)
1323 [10.1021/acs.est.9b05790, 2019.](#)
- 1324 Laurent, A., Fennel, K., Hu, J., & Hetland, R.: Simulating the effects of phosphorus limitation in
1325 the Mississippi and Atchafalaya river plumes. *Biogeosciences*, 9(11), 4707–4723.
1326 <https://doi.org/10.5194/bg-9-4707-2012>, 2012.
- 1327 Laurent, A., Fennel, K., Cai, W.-J., Huang, W.-J., Barbero, L., Wanninkhof, R.: Eutrophication-
1328 Induced Acidification of Coastal Waters in the Northern Gulf of Mexico: Insights into Origin
1329 and Processes from a Coupled Physical-Biogeochemical Model. *Geophys. Res. Lett.*, 44 (2),
1330 946–956. <https://doi.org/10.1002/2016GL071881>, 2017.
- 1331 Li, D., Zhang, J., Huang, D., Wu, Y., & Liang, J.: Oxygen depletion off the Changjiang (Yangtze
1332 River) Estuary. *Science in China Series D: Earth Science*, 45(12), 1137.
1333 <https://doi.org/10.1360/02yd9110>, 2002.
- 1334 Li, H. M., Tang, H. J., Shi, X. Y., Zhang, C. S., & Wang, X. L.: Increased nutrient loads from the
1335 Changjiang (Yangtze) River have led to increased Harmful Algal Blooms. *Harmful Algae*, 39,
1336 92–101. <https://doi.org/10.1016/j.hal.2014.07.002>, 2014.
- 1337 Li, M., Lee, Y. J., Testa, J. M., Li, Y., Ni, W., Kemp, W. M., & Di Toro, D. M.: What drives
1338 interannual variability of hypoxia in Chesapeake Bay: Climate forcing versus nutrient loading?
1339 *Geophysical Research Letters*, 43(5), 2127–2134. <https://doi.org/10.1002/2015GL067334>,
1340 2016.
- 1341 Li, X., Bianchi, T. S., Yang, Z., Osterman, L. E., Allison, M. A., DiMarco, S. F., & Yang, G.:
1342 Historical trends of hypoxia in Changjiang River estuary: Applications of chemical biomarkers
1343 and microfossils. *Journal of Marine Systems*, 86(3–4), 57–68, 2011.
1344 <https://doi.org/10.1016/j.jmarsys.2011.02.003>
- 1345 Liu, K. K., Yan, W., Lee, H. J., Chao, S. Y., Gong, G. C., & Yeh, T. Y.: Impacts of increasing
1346 dissolved inorganic nitrogen discharged from Changjiang on primary production and seafloor
1347 oxygen demand in the East China Sea from 1970 to 2002. *Journal of Marine Systems*, 141,
1348 200–217. <https://doi.org/10.1016/j.jmarsys.2014.07.022>, 2015.
- 1349 Liu, S. M., Hong, G.-H., Ye, X. W., Zhang, J., & Jiang, X. L.: Nutrient budgets for large Chinese
1350 estuaries and embayment. *Biogeosciences Discussions*, 6(1), 391–435.
1351 <https://doi.org/10.5194/bgd-6-391-2009>, 2009.
- 1352 Liu, S. M., Zhang, J., Chen, H. T., Wu, Y., Xiong, H., & Zhang, Z. F.: Nutrients in the
1353 Changjiang and its tributaries. *Biogeochemistry*, 62(1), 1–18, 2003.

Deleted: 2

1355 Locarnini, R. A., Mishonov, A. V., Antonov, J. I., Boyer, T. P., Garcia, H. E., Baranova, O.
1356 K., ... Seidov, D.: World Ocean Atlas 2013. Vol. 1: Temperature. S. Levitus, Ed.; A.
1357 Mishonov, Technical Ed.; NOAA Atlas NESDIS, 73, 40. [https://doi.org/10.1182/blood-2011-](https://doi.org/10.1182/blood-2011-06-357442)
1358 [06-357442](https://doi.org/10.1182/blood-2011-06-357442), 2013.

1359 Ni, X., Huang, D., Zeng, D., Zhang, T., Li, H., & Chen, J.: The impact of wind mixing on the
1360 variation of bottom dissolved oxygen off the Changjiang Estuary during summer. *Journal of*
1361 *Marine Systems*, 154, 122–130. <https://doi.org/10.1016/j.jmarsys.2014.11.010>, 2016.

1362 Ning, X., Lin, C., Su, J., Liu, C., Hao, Q., & Le, F.: Long-term changes of dissolved oxygen,
1363 hypoxia, and the responses of the ecosystems in the East China Sea from 1975 to 1995. *Journal*
1364 *of Oceanography*, 67(1), 59–75. <https://doi.org/10.1007/s10872-011-0006-7>, 2011.

1365 Peña, A., Katsev, S., Oguz, T., & Gilbert, D.: Modeling dissolved oxygen dynamics and hypoxia.
1366 *Biogeosciences*, 7(3), 933–957. <https://doi.org/10.5194/bg-7-933-2010>, 2010.

1367 Qian, W., Dai, M., Xu, M., Kao, S. ji, Du, C., Liu, J., ... Wang, L.: Non-local drivers of the
1368 summer hypoxia in the East China Sea off the Changjiang Estuary. *Estuarine, Coastal and*
1369 *Shelf Science*, 1–7. <https://doi.org/10.1016/j.ecss.2016.08.032>, 2015.

1370 Quiñones-Rivera, Z. J., Wissel, B., Justić, D., & Fry, B.: Partitioning oxygen sources and sinks in
1371 a stratified, eutrophic coastal ecosystem using stable oxygen isotopes. *Marine Ecology*
1372 *Progress Series*, 342, 69–83. <https://doi.org/10.3354/meps342069>, 2007.

1373 Rabalais, N. N., Díaz, R. J., Levin, L. A., Turner, R. E., Gilbert, D., & Zhang, J.: Dynamics and
1374 distribution of natural and human-caused hypoxia. *Biogeosciences*, 7, 585–619.
1375 <https://doi.org/10.5194/bg-7-585-2010>, 2010.

1376 [Scavia, D., Bertani, I., Obenour, D. R., Turner, R. E., Forrest, D. R. & Katin, A.: Ensemble](#)
1377 [modeling informs hypoxia management in the northern Gulf of Mexico, P. Natl. Acad. Sci.](#)
1378 [USA, 114, 8823–8828, 2017.](#)

1379 Scully, M. E.: Physical controls on hypoxia in Chesapeake Bay: A numerical modeling study.
1380 *Journal of Geophysical Research: Oceans*, 118(3), 1239–1256,
1381 <https://doi.org/10.1002/jgrc.20138>, 2013.

1382 [Smolarkiewicz, P. K., & Margolin, L. G.: MPDATA: A finite-difference solver for geophysical](#)
1383 [flows. Journal of Computational Physics, 140, 459-480, 1998.](#)

1384 Song, G., Liu, S., Zhu, Z., Zhai, W., Zhu, C., & Zhang, J.: Sediment oxygen consumption and
1385 benthic organic carbon mineralization on the continental shelves of the East China Sea and the
1386 Yellow Sea. *Deep-Sea Research Part II: Topical Studies in Oceanography*, 124, 53–63.
1387 <https://doi.org/10.1016/j.dsr2.2015.04.012>, 2016.

1388 Tong, Y., Zhao, Y., Zhen, G., Chi, J., Liu, X., Lu, Y., ... Zhang, W.: Nutrient Loads Flowing into
1389 Coastal Waters from the Main Rivers of China (2006–2012). *Scientific Reports*, 5, 16678.
1390 <https://doi.org/10.1038/srep16678>, 2015.

1391 Umlauf, L., & Burchard, H.: A generic length-scale equation for geophysical. *Journal of Marine*
1392 *Research*, 61(2), 235–265. <https://doi.org/10.1357/002224003322005087>, 2003.

1393 Wang, B.: Hydromorphological mechanisms leading to hypoxia off the Changjiang estuary.
1394 *Marine Environmental Research*, 67(1), 53–58,
1395 <https://doi.org/10.1016/j.marenvres.2008.11.001>, 2009.

1396 Wang, B., Wei, Q., Chen, J., & Xie, L.: Annual cycle of hypoxia off the Changjiang (Yangtze
1397 River) Estuary. *Marine Environmental Research*, 77, 1–5,
1398 <https://doi.org/10.1016/j.marenvres.2011.12.007>, 2012.

1399 Wang, B., Chen, J., Jin, H., Li, H., Huang, D., & Cai, W.-J.: Diatom bloom-derived bottom water
1400 hypoxia off the Changjiang Estuary, with and without typhoon influence, *Limnology and*
1401 *Oceanography*, 62, 1552–1569, <https://doi.org/10.1002/lno.10517>, 2017.

1402 Wang, H., Dai, M., Liu, J., Kao, S. J., Zhang, C., Cai, W. J., ... Sun, Z.: Eutrophication-Driven
1403 Hypoxia in the East China Sea off the Changjiang Estuary. *Environmental Science and*
1404 *Technology*, 50(5), 2255–2263. <https://doi.org/10.1021/acs.est.5b06211>, 2016.

1405 Wang, J., Yan, W., Chen, N., Li, X., & Liu, L.: Modeled long-term changes of DIN:DIP ratio in
1406 the Changjiang River in relation to Chl- α and DO concentrations in adjacent estuary. *Estuarine,*
1407 *Coastal and Shelf Science*, 166, 153–160. <https://doi.org/10.1016/j.ecss.2014.11.028>, 2015.

1408 Wei, H., He, Y., Li, Q., Liu, Z., & Wang, H.: Summer hypoxia adjacent to the Changjiang
1409 Estuary. *Journal of Marine Systems*, 67(3–4), 292–303,
1410 <https://doi.org/10.1016/j.jmarsys.2006.04.014>, 2007.

1411 Wei, H., Luo, X., Zhao, Y., & Zhao, L.: Intraseasonal variation in the salinity of the Yellow and
1412 East China Seas in the summers of 2011, 2012, and 2013. *Hydrobiologia*, 754(1), 13–28.
1413 <https://doi.org/10.1007/s10750-014-2133-9>, 2015.

1414 Wu, R. S. S.: Hypoxia: From molecular responses to ecosystem responses. *Marine Pollution*
1415 *Bulletin*, 45(1–12), 35–45. [https://doi.org/10.1016/S0025-326X\(02\)00061-9](https://doi.org/10.1016/S0025-326X(02)00061-9), 2002.

1416 Yu, L., Fennel, K., & Laurent, A.: A modeling study of physical controls on hypoxia generation
1417 in the northern Gulf of Mexico. *Journal of Geophysical Research C: Oceans*, 120(7), 5019–
1418 5039. <https://doi.org/10.1002/2014JC010634>, 2015a.

1419 Yu, L., Fennel, K., Laurent, A., Murrell, M. C., & Lehrter, J. C.: Numerical analysis of the
1420 primary processes controlling oxygen dynamics on the Louisiana shelf. *Biogeosciences*, 12(7),
1421 2063–2076. <https://doi.org/10.5194/bg-12-2063-2015>, 2015b.

1422 Yuan, D., Zhu, J., Li, C., & Hu, D.: Cross-shelf circulation in the Yellow and East China Seas
1423 indicated by MODIS satellite observations. *Journal of Marine Systems*, 70(1–2), 134–149.
1424 <https://doi.org/10.1016/j.jmarsys.2007.04.002>, 2008.

1425 Zhang, H., Zhao, L., Sun, Y., Wang, J., & Wei, H.: Contribution of sediment oxygen demand to
1426 hypoxia development off the Changjiang Estuary. *Estuarine, Coastal and Shelf Science*, 192,
1427 149–157. <https://doi.org/10.1016/j.ecss.2017.05.006>, 2017.

1428 Zhang, J.: Nutrient elements in large Chinese estuaries. *Continental Shelf Research*, 16(8), 1023–
1429 1045. [https://doi.org/10.1016/0278-4343\(95\)00055-0](https://doi.org/10.1016/0278-4343(95)00055-0), 1996.

1430 Zhao, L., & Guo, X.: Influence of cross-shelf water transport on nutrients and phytoplankton in
1431 the East China Sea: A model study. *Ocean Science*, 7(1), 27–43. [https://doi.org/10.5194/os-7-](https://doi.org/10.5194/os-7-27-2011)
1432 [27-2011](https://doi.org/10.5194/os-7-27-2011), 2011.

1433 Zheng, J., Gao, S., Liu, G., Wang, H., & Zhu, X.: Modeling the impact of river discharge and
1434 wind on the hypoxia off Yangtze Estuary. *Natural Hazards and Earth System Sciences*, 16(12),
1435 2559–2576. <https://doi.org/10.5194/nhess-16-2559-2016>, 2016.

1436 Zhou, F., Chai, F., Huang, D., Xue, H., Chen, J., Xiu, P., ... Wang, K.: Investigation of hypoxia
1437 off the Changjiang Estuary using a coupled model of ROMS-CoSiNE. *Progress in*
1438 *Oceanography*, 159, 237–254. <https://doi.org/10.1016/j.pocean.2017.10.008>, 2017.

1439 Zhou, F., Huang, D., Ni, X., Xuan, J., Zhang, J., & Zhu, K.: Hydrographic analysis on the multi-
1440 time scale variability of hypoxia adjacent to the Changjiang River Estuary. *Shengtai Xuebao/*
1441 *Acta Ecologica Sinica*, 30(17), 4728–4740, 2010.

1442 Zhu, J., Zhu, Z., Lin, J., Wu, H., & Zhang, J.: Distribution of hypoxia and pycnocline off the
1443 Changjiang Estuary, China. *Journal of Marine Systems*, 154, 28–40.
1444 <https://doi.org/10.1016/j.jmarsys.2015.05.002>, 2016.

1445 Zhu, Z.-Y., Zhang, J., Wu, Y., Zhang, Y.-Y., Lin, J., & Liu, S.-M.: Hypoxia off the Changjiang
1446 (Yangtze River) Estuary: Oxygen depletion and organic matter decomposition. *Marine*
1447 *Chemistry*, 125(1–4), 108–116. <https://doi.org/10.1016/j.marchem.2011.03.005>, 2011.

1448 Zweng, M. M., Reagan, J. R., Antonov, J. I., Mishonov, A. V., Boyer, T. P., Garcia, H. E., ...
1449 Bidlle, M. M., *World Ocean Atlas 2013, Volume 2: Salinity*. NOAA Atlas NESDIS (Vol. 119).
1450 <https://doi.org/10.1182/blood-2011-06-357442>, 2013.

1451

▼
▲
Page 11: [3] Deleted **Katja Fennel** **5/6/20 9:21:00 AM**

▼
▲
Page 11: [3] Deleted **Katja Fennel** **5/6/20 9:21:00 AM**

▼
▲
Page 11: [3] Deleted **Katja Fennel** **5/6/20 9:21:00 AM**

▼
▲
Page 11: [3] Deleted **Katja Fennel** **5/6/20 9:21:00 AM**

▼
▲
Page 11: [3] Deleted **Katja Fennel** **5/6/20 9:21:00 AM**

▼
▲
Page 11: [3] Deleted **Katja Fennel** **5/6/20 9:21:00 AM**

▼
▲
Page 11: [3] Deleted **Katja Fennel** **5/6/20 9:21:00 AM**

▼
▲
Page 11: [3] Deleted **Katja Fennel** **5/6/20 9:21:00 AM**

▼
▲
Page 11: [4] Deleted **Katja Fennel** **4/29/20 11:09:00 AM**

▼
▲
Page 11: [4] Deleted **Katja Fennel** **4/29/20 11:09:00 AM**

▼
▲
Page 11: [4] Deleted **Katja Fennel** **4/29/20 11:09:00 AM**

▼
▲
Page 24: [5] Deleted **Katja Fennel** **5/6/20 9:26:00 AM**

▼
▲
Page 26: [6] Deleted **Katja Fennel** **5/6/20 1:25:00 PM**